ATOMKI PREPRINT

A/23 (1987)

HU ISSN 0231-245X

FRAGMENTATION PROPERTIES OF ^{6}Li

R.G. Lovas, A.T. Kruppa, R. Beck and F. Dickmann

Submitted to Nuclear Physics A

May 1987

Institute of Nuclear Research of the Hungarian Academy of Sciences
Debrecen, P.O.Box 51, H-4001, Hungary

Kiadja a
Magyar Tudományos Akadémia
Atommagkutató Intézete
A kiadásért és szerkesztésért felelős
Dr.Berényi Dénes, az intézet igazgatója
Készült a Kinizsi Szakszövetkezet
Nyomdájában

FRAGMENTATION PROPERTIES OF ^{6}Li

R.G. Lovas and A.T. Kruppa

Kernforschungszentrum Karlsruhe, Institut für Kernphysik III,
P.O.Box 3640, D-7500 Karlsruhe 1, Federal Republic of Germany

and

Magyar Tudományos Akadémia Atommagkutató Intézete,
Debrecen, P.O.Box 51, H-4001, Hungary†

and

R. Beck* and F. Dickmann*

Kernforschungszentrum Karlsruhe, Institut für Kernphysik III,
P.O.Box 3640, D-7500 Karlsruhe 1, Federal Republic of Germany

Abstract. The α+d and t+τ cluster structure of ^{6}Li is described in a microscopic α+d cluster model through quantities that enter into the description of cluster fragmentation processes. The states of the separate clusters α, d, t and τ are described as superpositions of Os Slater determinants belonging to different potential size parameters. The model state space of ^{6}Li is a tensor product of the α and d cluster state spaces and the state space of zero-orbital-momentum relative motion, restricted by antisymmetrization. To describe both the ^{6}Li and fragment states realistically, we constructed nucleon-nucleon forces optimized for the model state spaces used. The fragmentation properties calculated are the g.s. fragmentation

(or reduced-width) amplitudes, their squared Fourier transforms, the corresponding potential overlaps, the spectroscopic factors $S_{\alpha d}$, $S_{t\tau}$ and the αd asymptotic normalization constant $\tilde{C}_{\alpha d}$. The forces constructed reproduce the energies and charge radii of ^{6}Li as well as of the fragments excellently. The fragmentation properties predicted by them slightly differ from those calculated with some forces of common use provided the latter are modified so as to reproduce the α, d and ^{6}Li energies. The fragmentation properties change moderately in comparison with simpler versions of the cluster model. The full model yields $S_{\alpha d}$=0.93, $S_{t\tau}$=0.58 and $\tilde{C}_{\alpha d}$=3.3. The results are consistent with phenomenological estimates except for $\tilde{C}_{\alpha d}$. The shapes of our αd fragmentation amplitudes are in accord with α+p+n three-body calculations but our $S_{\alpha d}$ and $\tilde{C}_{\alpha d}$ are substantially larger. We attribute this discrepancy to the neglect of the Pauli effects in the usual three-body formula for the αd fragmentation amplitude. We give a formula which contains the necessary remedy.

---

† Present and permanent address.

* Deceased.

1. Introduction

It has been a challenge for some time both for experimentalists and theoreticians to understand the cluster structure of the nucleus ^{6}Li. The main experimental tool invoked is quasielastic cluster knock-out reactions[1]), while the theoretical efforts embrace all versions of the cluster model[2]). It has been conjectured that the g.s. of ^{6}Li is dominated by the two overlapping[2,3]) configurations α+d and t+τ (τ=^{3}He). This initiated the use of four-nucleon[1]) and, to a lesser extent, three-nucleon[4]) transfer reactions from ^{6}Li to probe the cluster structure of other nuclei.

The link between the models of knock-out, transfer as well as direct radiative capture[5]) reactions and structure theory is most conveniently[6]) established through the fragmentation amplitudes (or reduced-width amplitudes), which are the overlaps of the g.s. nuclear wave function with those of the free fragments. The norm squares of the fragmentation amplitudes, the so-called spectroscopic factors, are used to characterize the fragmentation properties in an integrated form.

The fragmentation properties of ^{6}Li have been studied in microscopic as well as semi-microscopic models. The former include the harmonic-oscillator (h.o.) α+d model[3]) and dynamical cluster models, which assume a pure {α+d}[7]) and the mixed {α+d,α+d*}[8]) or {α+^{3}He+p}[9,10]) configurations, while the latter include the α+p+n three-body models[11-15]). There is a systematic difference between the predictions of these two types of models. While the microscopic models give αd spectroscopic factors ($S_{\alpha d}$) around unity, the three-body models yield $S_{\alpha d}$ =0.5 ÷ 0.75.

The experimental estimates cannot decide between these two predictions. The results of recent high-energy (E >> 100 MeV) kinematically complete quasi-free knock-out experiments support the microscopic models. In particular, the (p,pd) data of Kitching et al.[16]) (E =590 MeV) reanalysed[17]) result in $S_{\alpha d}$=1.08, the (α,2α) data of Dollhopf et al.[17]) (E =700 MeV) yield $S_{\alpha d}$=1.05, and the (p,pd) data of Albrecht et al.[18]) (E =670 MeV) give $S_{\alpha d}$=1.08. The radiative capture experiment of Robertson et al.[19]) takes a medium position with $S_{\alpha d}$=0.85. The lower-energy (E =100 MeV) (p,pα) data of Roos et al.[20]), however, lean towards the three-body models ($S_{\alpha d}$=0.58). Further information on the spectroscopic factor is obtained by a requirement of consistency with the values of the asymptotic normalization constant extracted from elastic scattering. This requirement leads[21]) to $S_{\alpha d}$=0.42, which, again, favours the three-body models. As to t+τ clustering, the relevant (i.e. microscopic) models yield[3,10]) values $S_{t\tau} \approx 0.5\, S_{\alpha d}$, while the analyses of experiments do not exclude an opposite relationship. Namely, the comparative analyses of (p,pα) and (p,pτ) experiments by Roos et al.[22]) produce $S_{t\tau}=0.73\, S_{\alpha d}$ or $S_{t\tau}=1.35\, S_{\alpha d}$ depending on the assumed shape of the fragmentation amplitudes. Furthermore, the radiative capture data of Young et al.[23]) and Ventura et al.[24]) yield the surprisingly high values of $S_{t\tau}$=0.69 and 0.79, respectively.

The discrepancies between these experimental results are genuine as the experimental errors are mostly below 10 %. The discrepancies may come partly from uncertainties in the reaction mechanism. It was in order to purify the reaction mechanism that, very recently, electron bombardment was used by Ent et al.[25]) to

bring about knock-out reaction. Their (e,ed) experiment, performed at E=480 MeV, resulted in $S_{\alpha d}$=0.73±0.09. Most analyses of knock-out[26]) and radiative capture reactions rely upon assumptions on the shape of the fragmentation amplitude, just as transfer reactions[27]) do. In fact, some tests[22,26,27]) show that these analyses depend critically on these assumptions. Better justified assumptions can only be based on better theoretical calculations. Improved theoretical calculations of the fragmentation amplitudes are thus needed not just to understand the experimental estimates of these functions but also to help further analyses of experimental data.

Our aim in this paper is to provide an improved microscopic calculation for the characteristics of the fragmentation. In our earlier work[9]) we found that the admixture of ^{5}He+p clusterization to the α+d component has little effect not only on the g.s. energy but also on the α+d fragmentation properties. On the other hand, we found that the energy can be improved substantially by including the breathing excitations[28]) of α and d. It is thus important to see what changes in the fragmentation amplitudes are caused by this improvement on the model, and that is the subject of this paper.

The physical ingredients of the model are summarized in sect.2. To produce good estimates for the fragmentation properties, the description of the separate fragments also has to be realistic and consistent with that of the composite system. Interactions that satisfy this strict condition are presented in sect.3. The results are presented in sect.4 and are further discussed in sect.5.

2. The model

A general description of our model in technical terms was given in ref.[28]). Here we only recall its essentials to expose the forthcoming considerations and to explain our notation. We choose a different presentation now to elucidate the physical aspects of our concern.

To describe ^{6}Li, our model uses the wave-function ansatz

$$\Psi = \sum_{k\ell} \mathcal{A}\{\psi_k(\alpha)\psi_\ell(d)\chi_{k\ell}(r_{\alpha d})\}, \qquad (2.1)$$

where ψ and χ depend on the cluster internal and relative coordinates, respectively. The functions ψ are antisymmetrized and $\mathcal{A} = N^{-1/2}\Sigma_p(-)^p P$ is the rest-antisymmetrizer, where N is the number of terms in $\mathcal{A}$ (for α+d, N=6!/4!2!). If the sum in (2.1) runs over a complete set of cluster intrinsic states and χ are chosen appropriately, (2.1) may be an exact expansion. A reasonable and tractable truncation should keep the g.s.'s of the independent clusters, $\psi_1(\alpha)$ and $\psi_1(d)$, and, to allow for the distortion of the clusters in each other's field, a few excited states. If the d-state admixtures, are neglected, as they will be, the spatial parts of both functions ψ are spherically symmetric.

To construct the functions ψ, we solve the problems of the free clusters A=α,d on a basis $\{\phi_m(A)\}$ of translation invariant antisymmetrized 0s h.o. states of different size parameters β_m^A = $M_{\text{nucleon}}\omega_m^A/\hbar$:

$$\psi_m(A) = \sum_{n=1}^{N_A} c_{mn}^{(A)}\,\phi_n(A) \qquad (m = 1, .., N_A;\ A=\alpha,\ d). \qquad (2.2)$$

The basis states $\phi_n(A)$ are related to the corresponding Slater determinants $\tilde{\phi}_n(A,\underset{\sim}{s}^A)$ centred around $\underset{\sim}{s}^A$ as

$$\tilde{\phi}_n(A,\underset{\sim}{s}^A)=(A\beta_n^A/\pi)^{3/4}\exp\{-\tfrac{1}{2}A\beta_n^A(\underset{\sim}{x}^A-\underset{\sim}{s}^A)^2\}\,\phi_n(A)\,, \tag{2.3}$$

where $\underset{\sim}{x}^A$ is the c.m. coordinate of cluster A of mass number A. Inserting (2.2) in (2.1), we get

$$\Psi=\sum_{i,j}\mathcal{A}\{\phi_i(\alpha)\phi_j(d)\gamma_{ij}(\underset{\sim}{x}_{\alpha d})\}\,, \tag{2.4}$$

with $\gamma_{ij}(\underset{\sim}{x}_{\alpha d})=\sum_{kl}c_{ki}^{(\alpha)}c_{lj}^{(d)}\chi_{kl}(\underset{\sim}{x}_{\alpha d})$ and $\underset{\sim}{x}_{\alpha d}=\underset{\sim}{x}^d-\underset{\sim}{x}^\alpha$. We approximate γ_{ij} with a combination of orbital-momentum projected shifted gaussians centred around a set of discrete points $\underset{\sim}{s}_k$,

$$\gamma_{ij}(\underset{\sim}{x}_{\alpha d})=\sum_k f_{ijk}\int d\hat{\underset{\sim}{s}}_k\,Y_{L\Lambda}(\hat{\underset{\sim}{s}}_k)\,\varphi_{ij}(\underset{\sim}{x}_{\alpha d}-\underset{\sim}{s}_k)\,, \tag{2.5}$$

where

$$\varphi_{ij}(\underset{\sim}{s})=\left(4\frac{4\beta_i^\alpha 2\beta_j^d}{(4\beta_i^\alpha+2\beta_j^d)^2}\right)^{3/4}\exp\left(-\frac{1}{2}\frac{4\beta_i^\alpha 2\beta_j^d}{4\beta_i^\alpha+2\beta_j^d}\,\underset{\sim}{s}^2\right). \tag{2.6}$$

(For simplicity, we suppress the coupling of the spin with the orbital momentum.) It is now useful to employ the identity

$$\varphi_{ij}(\underset{\sim}{x}_{\alpha d}-\underset{\sim}{s})=[4\beta_i^\alpha 2\beta_j^d/\pi^2]^{3/4}\int d\underset{\sim}{\xi}\exp\{-\tfrac{1}{2}[4\beta_i^\alpha(\underset{\sim}{x}^\alpha-\underset{\sim}{s}^\alpha)^2+2\beta_j^d(\underset{\sim}{x}^d-\underset{\sim}{s}^d)^2]\}\,, \tag{2.7}$$

where $\underset{\sim}{\xi}=\frac{4}{6}\underset{\sim}{s}^\alpha+\frac{2}{6}\underset{\sim}{s}^d$, $\underset{\sim}{s}=\underset{\sim}{s}^d-\underset{\sim}{s}^\alpha$ and $\underset{\sim}{x}^\alpha$, $\underset{\sim}{x}^d$ are any vectors obeying $\underset{\sim}{x}^d-\underset{\sim}{x}^\alpha=\underset{\sim}{x}_{\alpha d}$, so they may be identified with the cluster c.m. coordinates introduced in (2.3). Substituting (2.7) into (2.5) and (2.5) into (2.4), and using (2.3), we obtain

$$\Psi=\sum_{ijk}f_{ijk}\Phi_{ijk}\,, \tag{2.8}$$

with

$$\Phi_{ijk}=\int d\hat{\underset{\sim}{s}}_k\,Y_{L\Lambda}(\hat{\underset{\sim}{s}}_k)\int d\underset{\sim}{\xi}\,\tilde{\Phi}_{ijk}\,, \tag{2.9}$$

where

$$\tilde{\Phi}_{ijk}=\mathcal{A}\{\tilde{\phi}_i(\alpha,\underset{\sim}{s}_k^\alpha)\tilde{\phi}_j(d,\underset{\sim}{s}_k^d)\}\,. \tag{2.10}$$

Eq.(2.8) contains a linear combination of functions Φ_{ijk} characterized by different values of the three parameters β^α, β^d and $\underset{\sim}{s}$. Thus, Ψ can be regarded as the trial function of the generator-coordinate (GC) method (GCM) with the three GC's β^α, β^d, $s=|\underset{\sim}{s}|$ discretized. The model requires the solution of the Hill-Wheeler equation

$$\sum_{i'j'k'}\left(\langle\Phi_{ijk}|H|\Phi_{i'j'k'}\rangle-E\langle\Phi_{ijk}|\Phi_{i'j'k'}\rangle\right)f_{i'j'k'}=0\,. \tag{2.11}$$

One can recognize that Φ_{ijk} are expressed in terms of Slater determinants, so that the normalization and hamiltonian kernels, $\langle\Phi_{ijk}|\Phi_{i'j'k'}\rangle$ and $\langle\Phi_{ijk}|H|\Phi_{i'j'k'}\rangle$, may be calculated with the well-known GC techniques[29]. It is seen that the translation invariant basis states Φ_{ijk} are related to the Slater determinants $\tilde{\Phi}_{ijk}$ through an integration over $\underset{\sim}{\xi}$. Since $\underset{\sim}{\xi}$ is a common displacement vector of the two clusters, this integration can be interpreted as a Peierls-Yoccoz momentum projection[30] to c.m. momentum zero.

The problem of each separate cluster, formulated in (2.2), leads to an equation similar to (2.11), with the single GC $\beta^A=\beta^\alpha$ or $\beta^A=\beta^d$.

With the expansions (2.2), the assumption (2.1) amounts to allowing for three degrees of freedom: the breathing vibrations and the relative motion of the two clusters. Thus the physical ingredients of our model are not different from other versions of the cluster distortion models[31]. It would add to the heuristic appeal of the model if the clusters were seen to be explicity

deformed in each other's field[32]). It was shown, however, that the inclusion of cluster deformation is equivalent to inclusion of a combination of one-particle one-hole cluster excitations that has a large overlap with a breathing excitation[33]).

In order that (2.1) may represent the breathing-cluster picture faithfully, the sets of states $\{\phi_n(A), n=1,\dots,N_A\}$ $(A=\alpha,d)$ and $\{\varphi_{ij}(\vec{r}_{\alpha d}-\vec{s}_k),\ k=1,\dots,N_s\}$ should be reasonably complete. To this end, we optimized the choice of the discretized values of the GC's. For $\{\beta^A_n\}$ such an optimization may be viewed as a generalization of the often quoted stability condition[31]), and was indeed found very effective. E.g., with the Volkov 2 (V2) force[34]) the g.s. energy of the deuteron with 14 equidistant β^d values is $E_d = -0.600$ MeV [ref.[28])], while 5 optimized values yield $E_d = -0.6076$ MeV, in fair agreement with the exact value, $E_d = -0.6082$ MeV. In general, to achieve a convergence of E_d, E_t, E_τ and E_α within 1 ÷ 2 keV, it was sufficient to take $N_d=5$, $N_t=N_\tau=4$ (with $\beta^t=\beta^\tau$) and $N_\alpha=3$. We adopted these values and the corresponding GC values for the two-cluster nuclei as well. A variation of the $\{s_n\}$ values in ^{6}Li showed that an equidistant set is near the optimum, and the adopted set, 1,2,...,12 fm, is good enough to yield a similar accuracy.

It looks likely that the $L\neq 0$ admixtures to d and ^{6}Li play a minor role in the decomposition properties of ^{6}Li. We therefore used central forces.

The breathing cluster model comprises a range of simpler models as special cases, two of which will be considered here. By choosing $N_\alpha=N_d=1$, we get a model, which is equivalent to the conventional resonating group model (RGM) with no distortion. This

we shall call the "RGM-type" model. If, furthermore, we fix the single β^α to be equal to β^d, and choose it so as to minimize $E_\alpha+E_d$, we fall back to the conventional GCM ("GCM-type" model).

3. The interaction

3.1. *SURVEY OF FORCES OF COMMON USE*

The fragmentation of a nucleus is well-known to be very sensitive to the separation energy. In our case it is therefore important to reproduce $E_{\alpha d}=E(^6\text{Li})-E_\alpha-E_d$ and $E_{t\tau}=E(^6\text{Li})-E_t-E_\tau$. Thus the energies of the individual clusters should be correct, apart, possibly, from a constant shift, which should be compensated for by a similar shift in $E(^6\text{Li})$. We have found, however, that the αd fragmentation amplitude is sensitive to the size of d as well[10]), which, in turn, strongly depends on E_d, owing to the weak binding of d. This implies that all energies E_α, E_d, E_t, E_τ and $E(^6\text{Li})$ should be correct in an absolute sense. This imposes a very strict condition on the interaction to be used.

From this point of view, we have examined the interactions of common use. The forces considered are the Volkov forces[34]) (V1,...,V8) the Brink-Boeker forces[35]) B_1 and B_2, the modified version[36]) of force 2 of Hasegawa and Nagata[7]) (MHN) and three forces proposed by the Minnesota group, viz. those of Thompson and Tang[37,38]) (TT1 and TT2) and of Thompson, LeMere and Tang[39]) (TLT). The resulting binding energies and rms charge radii of the single-cluster nuclei are collected in table 1. In all these calculations the basis was optimized for each force.

It is seen that none of the forces reproduces all energies and radii satisfactorily. This is not surprising, since a calculation on a truncated model space always requires an effective interaction particular to the function space employed, and none of the forces considered here has been constructed so as to match just our model space. In particular, the Minnesota forces were constructed so as to imitate the interaction of the free nucleons. Thus they give realistic results for the deuteron, whose function space in our model is virtually complete, but not for the other single clusters. In order that such a force may give realistic results for the larger clusters as well, it has to show the correct nuclear saturation, which property also depends on the function space. The TT1 and TT2 forces are seen to overbind the α particle; in fact they show proper saturation in the more restricted space of a single h.o. model of realistic size parameter. The MHN force gives too large bindings for similar reasons. It is an effective force whose parameters were tuned so as to describe the deuteron in a single h.o. model. The Volkov and Brink-Boeker forces are effective forces devised for broader ranges of application. Considering that their parameters were extracted by fitting to the properties of larger nuclei and nuclear matter in completely different models, their performances may be said remarkably good. [The B_3 and B_4 interactions[35]), however, are not considered here because they grossly overbind the nuclei of our interest.]

It should be noted that the degrees of discrepancy in the energies and radii are correlated, especially for the deuteron. We tested this correlation by varying the overall strengths of the interactions. By making E_d correct in this way, we always

obtained reasonable values for the radius r_d as well. This finding points to the possibility of constructing interactions more suited to the cluster distortion models.

We used effective interactions of three types. Firstly, we constructed interactions by carefully deliberated optimization procedures. Secondly, to test the interactions of the first type against something more accepted, we compared them to modified versions of some of those given in table 1. And thirdly, to test to what extent our prescriptions hinge on the cluster distortion picture and to provide a basis of objective comparison with simpler cluster models, we constructed interactions appropriate for cluster models without distortion. These three types of interactions will be presented in subsections 2,3 and 4, respectively.

3.2. OPTIMIZED INTERACTIONS

We have seen that the interactions of common use do not reproduce all cluster energies and radii in the breathing model, but there is hope that more appropriate interactions can be constructed. Attempting this, we chose the potential form

$$V(i,j) = (W + M P_{ij}^{r} + B P_{ij}^{\sigma} - H P_{ij}^{\tau}) f(r_{ij}) , \qquad (3.1)$$

with

$$f(r) = \sum_{\nu=1}^{2} V_\nu \exp(-r^2/a_\nu^2) , \qquad (3.2)$$

where P_{ij}^{r}, P_{ij}^{σ} and P_{ij}^{τ} are the coordinate-, spin- and isospin-exchange operators, respectively.

It is easy to see that the potential kernels $\langle\phi_n|\sum_{i,j}V(i,j)|\phi_{n'}\rangle$ of the free Os clusters only depend on two combinations of the exchange mixtures,

$$\xi = W + M \quad \text{and} \quad \zeta = B + H. \tag{3.3}$$

In particular, the kernels of the singlet and triplet nucleon pairs are proportional to $\xi - \zeta$ and $\xi + \zeta$, respectively, while those of t, τ and α are proportional just to ξ. The form of (3.1) gives us freedom to fix $\xi + \zeta = 1$.

The nuclear potential kernel of a system of an α particle and another Os cluster depends on what the kernels of the constituents depend on and, in addition, on the combination

$$\eta = 4W - M + 2B - 2H. \tag{3.4}$$

For α+t(τ) this was noted by Brown and Tang[42], but, to our knowledge, it has not been observed in its full generality. We therefore prove this statement. The proof, relegated to the appendix, is constructive in that it sets up a most economical framework for calculating the potential kernels.

This behaviour of the kernels allows one to determine the potential parameters step by step. We determined ξ, V_1, V_2, a_1 and a_2 by fitting them to the measured energies and rms charge radii of the independent s-wave clusters simultaneously. In the course of this parameter fitting we also constructed the optimal cluster bases. In fact, because of the dependence of the optimum bases on the interaction, a basis optimization had to be carried through for each nucleus in each step of the variation of the force parameters. We then fixed η so as to have $E(^6\text{Li})$ or, for test purposes, $E(^7\text{Li})$ exact [$\eta = \eta(^6\text{Li})$ or $\eta = \eta(^7\text{Li})$]. [We included the Coulomb potential in the two-cluster calculations with the method described in ref.[43]).] One combination of the exchange mixtures remains undefined. This free parameter facilitates future applications for, depending on the problem, it can be adjusted e.g. to odd-L nucleon-nucleon phase shifts or to the energy of a more complicated nucleus.

The parameters of four versions of the force, each with the two different η, are given in table 2. We label them with symbol D to express that they are tailored for a distortion model. The forces D_1, D_2 and D_3 were constructed by fitting to the properties of d,t and α, of d,t,τ and α and of d,τ and α, respectively. The version D_2' is similar to D_2 but contains only Wigner and Majorana terms, just like the Volkov forces. It is interesting that the results are rather insensitive to whether ξ is smaller or larger than unity; even the constraint $\xi = 1$ applied in D_2' yields reasonable results. Obviously, in applications in which the singlet np pair plays a prominent role, a version, like D_3, in which $\xi < 1$, could only be expected to give reasonable results.

The energy and radius values produced by the D forces are contained in table 3. In the parameter search we found that it is easy to achieve arbitrary accuracy in the energies, but an exact reproduction of the radii would require more flexibility. The agreement is still reasonable for the radii as well except that the large difference between the measured r_τ and r_t, 0.18 or 0.28 fm, cannot be reproduced. In our model there is no way to shift $r_\tau - r_t$ from ≈0.02 fm.

The ^{6}Li radius values obtained by the D forces are more

accurate than those obtained with the forces of common use[44]). The D forces also reasonably reproduce the g.s. energies of ^{5}He, ^{7}Li, ^{7}Be and ^{8}Be and the energy of the first excited $L = 2$ triplet as well as the electromagnetic properties of ^{6}Li [45]).

3.3. STANDARD FORCES MODIFIED

Given the breathing cluster basis, the D forces appear superior to the standard forces discussed in sect. 3.1. Nevertheless, because of the ad hoc manner they were constructed, it seems desirable to test them against the standard forces. The standard forces considered have the form

$$V(i,j) = \sum_{\nu=1}^{3} (W_\nu + M_\nu P^\tau_{ij} + B_\nu P^\sigma_{ij} - H_\nu P^\tau_{ij} P^\sigma_{ij}) V_\nu \exp(-r^2/\alpha_\nu^2) . \qquad (3.5)$$

The tests should concern the fragmentation properties themselves. Since these are closely related to the energy values produced and the D forces produce the exact values by construction, the comparison will only be fair if the standard forces are also readjusted to some extent. The dependence of the potential matrix elements on the exchange mixtures allows one to set the deuteron, α-particle and ^{6}Li energies by readjusting $\xi_\nu + \zeta_\nu$ (or rather V_ν), ξ_ν and η_ν, consecutively.

The parameters of the modified forces (prefixed M) constructed in this way are given in table 4. In the cases of the V1, V2 and V7 potentials, whose terms ν have common mixture parameters, we simply renormalized V_ν, ξ_ν and η_ν independent of ν. For the B_1, B_2 and MHN potentials all V_ν and ξ_ν were renormalized, but the ^{6}Li energy was set by changing η_1 only. The treatment of the TLT force

was somewhat different. This force yields nearly exact E_d, and thus no provision was needed for E_d. Complying with the convenient form of the TLT force,

$$V(i,j) = [V_1 f_1(r) + \tfrac{1}{2}(1+P^\sigma_{ij}) V_2 f_2(r) + \tfrac{1}{2}(1-P^\sigma_{ij}) V_3 f_3(r)] [\tfrac{1}{2} u + (2-u) P^\tau_{ij}] , \qquad (3.6)$$

we set E_α and $E(^6\mathrm{Li})$ by readjusting V_3 and u, respectively.

The energies and radii calculated with the M forces are also displayed in table 3. We see that the predicted values, viz. the three-nucleon energies and all radii, are mostly reasonable though they are, of course, less good in most cases than the values obtained with the D forces.

3.4. INTERACTIONS FOR THE RESTRICTED MODELS

The simplifications involved in the restricted models change the energies and hence spoil the fragmentation properties. This may only be offset by changing the interaction at the same time. We attempted to construct interactions, of the form of the D forces, that are suitable for the "RGM-type" model. We found, however, that there is not enough freedom in this interaction to describe the deuteron and the other single-cluster nuclei simultaneously in this model. We therefore included one more free parameter by allowing ξ_2 to be different from ξ_1. The parameters of the resulting force R are given in table 5; its predictions for the energies and radii can be found in table 3.

We also tried to tailor one of the standard forces, V2, for the "RGM-type" model. The force patterned upon the MV2 force yields, however, an unrealistic deuteron radius (1.66 fm), and

therefore we dismissed this idea. In this model the sizes of the separate clusters are obtained to be more realistic even with the use of the original V2 force. This gave us the idea of replacing the requirement of the correct binding energies with that of the correct separation energy $E_{\alpha d}$. This can be easily fulfilled by a simple adjustment of η or, equivalently, of the Majorana parameter M. It is this prescription that we adopted for calculations in the GCM-type model as well. The values of the M parameter of the V2 force that yield the correct separation energy in the "RGM-" and "GCM-type" models are 0.46091 and 0.57573, respectively. The calculated properties of the free clusters are again included in table 3.

4. Fragmentation properties

4.1. DEFINITIONS

In this paper we only consider the fragmentation of the g.s. of ^{6}Li into the g.s.'s of the α+d and t+τ fragments. We now present fragmentation amplitudes, fragmentation strengths, potential overlaps, spectroscopic factors and asymptotic normalization constants. We had presented calculations for the amounts of clustering and for fragmentation from and into excited states elsewhere[9,10].

The a+b (=α+d or t+τ) fragmentation amplitude is defined in configuration space as

$$G_{ab}(\underline{r}) \equiv r^{-1} g_{ab}(r) Y_{00}(\hat{\underline{r}}) = \langle \mathcal{A}\{\psi_1(a)\psi_1(b)\,\delta(\underline{r}-\underline{r}_{ab})\}|\Psi\rangle . \qquad (4.1)$$

This function appears in Born and impulse-type approximations to the transition amplitudes of cluster fragmentation processes[6,43]. In a plane-wave impulse approximation the ^{6}Li(c,ca)b-type knock-out transition amplitude is just proportional to the Fourier transform

$$\tilde{G}_{ab}(k) \equiv \tilde{g}_{ab}(k) Y_{00}(\hat{k}) = \int d\underline{r}\,(2\pi)^{-3/2}\, e^{i\underline{k}\underline{r}}\, G_{ab}(\underline{r}) . \qquad (4.2)$$

Thus the function

$$f_{ab}(k) = (4\pi)^{-1} \left|\tilde{g}_{ab}(k)\right|^2 , \qquad (4.3)$$

which we call the fragmentation strength[9], may be extracted directly from the cross section in this approximation. The potential overlap, defined as

$$W_{ab}(\underline{r}) \equiv r^{-1} w_{ab}(r) Y_{00}(\hat{\underline{r}}) = \langle \mathcal{A}\{\psi_1(a)\psi_1(b)\delta(\underline{r}-\underline{r}_{ab}) \sum_{i\in a}\sum_{j\in b} \ldots(i,j)\}|\Psi\rangle , \qquad (4.4)$$

enters into the description of (^{6}Li,a) and (^{6}Li,b) reactions in the post form of the distorted-wave Born approximation[43].

We also calculate the spectroscopic factor

$$S_{ab} = \int d\underline{r}\,|G_{ab}(\underline{r})|^2 = \int d\underline{k}\,|\tilde{G}_{ab}(k)|^2 \qquad (4.5)$$

and the asymptotic normalization constant[46]

$$\bar{C}_{ab} = \lim_{r\to\infty} \frac{1}{(2\varkappa)^{1/2}} \frac{g_{ab}(r)}{W_{-\eta,L+\frac{1}{2}}(2\varkappa r)} \qquad (L=0), \qquad (4.6)$$

where $\varkappa$ is the asymptotic wave number of the ab relative motion, η is the Sommerfeld parameter of the ab Coulomb interaction and W is the Whittaker function. The constant $\bar{C}_{ab}$ can be determined e.g. from a+b elastic scattering data.

We calculated the amplitudes $g_{ab}(r)$ analytically using the direct evaluation method based on Jacobi coordinates as is given in ref.[47]). The Fourier transformation was also performed analytically. The potential overlap was calculated analytically with the equation-of-motion method[47]).

All these fragmentation properties are interrelated and show parallel variations between the different models and forces. It is thus not necessary to present all of them for all these cases. Since the amplitude $g_{ab}(r)$ seems to be the most fundamental of these quantities and, through its close similarity to an inter-cluster "relative wave function" [10]), its meaning seems the most transparent, we shall carry through all comparisons in terms of such amplitudes. Furthermore, since both the model and its submodels are tailored primarily for the investigation of the α+d structure, their comparison for the t+τ fragmentation is less rich in implications. Therefore, we shall illustrate the t+τ properties more sparingly.

In subsect. 4.2 we compare the αd fragmentation amplitudes as predicted by the breathing cluster model and its submodels. In subsect. 4.3 we present calculations for all of the αd and tτ fragmentation properties in order to compare the results with phenomenology. For the fragmentation amplitudes and potential overlaps phenomenology will be represented by local-potential models used to analyse cluster transfer reactions. The fragmentation strengths will be directly compared with knock-out data as interpreted in the plane-wave impulse approximation. The subsection will be concluded with a comparison of the calculated spectroscopic factors and asymptotic normalization constant with various phenomenological estimates.

4.2. DEPENDENCE ON PHYSICAL INGREDIENTS

In this subsection we shall illustrate the force and model dependence of the fragmentation properties through examples for the αd fragmentation amplitudes.

In fig. 1 we show $g_{\alpha d}(r)$ as given by the breathing cluster model combined with the D_1, D_2, D_2' and D_3 forces. In fact, the resolution of the figure does not allow to distinguish the curves produced by D_2 and D_2'. Fig. 2 shows $g_{\alpha d}(r)$ calculated with representatives of the M forces, and, for the sake of comparison, with D_2. The results with the M forces that are not shown here are simple to summarize. The $g_{\alpha d}(r)$ functions produced by the MV1 and MV7 forces compare with the MV2 curve much the same as the D_1 and D_2 curves do with D_3. The MB_2 curve also runs pretty close to its kin, MB_1, while the MMHN curve is virtually indistinguishable from the MTLT one.

It is due to note here that the relationship between the tτ fragmentation amplitudes is very similar to that between the αd ones. We can thus assert that the dependence of the fragmentation amplitudes in the breathing cluster model on the choice of the force is not significant provided the forces produce realistic energies and radii. The slight differences appear mostly in the "extension" of the function as may be characterized e.g. by the position of the node. Conferring with table 3, one can observe a strict parallelism between the change of the ^{6}Li radius and the shift of the node of $g_{\alpha d}(r)$. Since the experimental radius is reproduced most accurately by the D forces, it seems justifiable to regard the D forces as the most realistic ones for the fragmentation properties as well.

The model dependence of $g_{\alpha d}$ is illustrated in fig. 3. Here we chose the breathing model with the MV2 force as the reference case, and we test the restricted models with the interactions introduced in sect. 3.4. We see that there is a definite model dependence. The "GCM-type" model with the V2 force (adjusted in η to give the correct α+d separation energy) gives a result substantially different from the "RGM-type" model with the same force (although it is readjusted). The discrepancy between the "RGM--type" model and the full model is much less. Moreover, the force R, tailored for the "RGM-type" model, gives almost the same $g_{\alpha d}(r)$ as the V2 force in the same model. We can thus interpret the difference of these two from the MV2 results as a genuine difference between the "RGM-type" and the breathing model. We can see that this difference is less significant than that caused by the incorrect size of the deuteron in the "GCM-type" model. We should add that the model dependence of $g_{t\tau}(r)$ is also very similar to that of $g_{\alpha d}(r)$.

Having seen the model dependence of $g_{\alpha d}$ with energetically adjusted forces, it will be easier to appreciate the role of this adjustment. In fig. 4 the MV2 result is contrasted with four curves calculated with the original V2 force ($M = 0.6$): one in the breathing model, one in the "RGM-type" model and two in the "GCM--type" model, one of which calculated without the Coulomb force. We see that the differences are substantially larger than between similar but energetically consistent $g_{\alpha d}$ results. Moreover, the smallest deviation from the MV2 curve is produced just by the roughest model, the "GCM-type" model without Coulomb force. This is so because the discrepancy in $g_{\alpha d}(r)$ is closely associated with

the extent of disagreement in $E_{\alpha d}$ (see the caption of fig. 4). Being a <u>difference</u> of binding energies, the value of $E_{\alpha d}$ is not informative of the quality of the approximation. It is to eliminate this accidental element that the forces have been readjusted in all other cases.

Other test calculations reveal that the cluster internal energies have their effect primarily through the cluster size. But, as we have seen in sect. 3.1, the cluster size is closely correlated with the energy, unless unphysical constraints are imposed upon the bases $\{\phi_\alpha(\alpha)\}, \{\phi_d(d)\}$, which would lead to spuriously large distortion effects[31]). Another interesting observation is that the $g_{t\tau}$ amplitude is more sensitive to $E_{\alpha d}$ than to $E_{t\tau}$ itself. All these facts indicate that no reliable estimates can be made for the fragmentation properties without the description of the nucleus and each pair of fragments being correct simultaneously.

4.3. COMPARISON WITH PHENOMENOLOGY

Due mainly to the accessibility of the α+d structure to experiment, the phenomenological estimates and models for the αd relative motion are numerous. We have recently reviewed both the transfer--reaction[48]) and knockout-reaction[9]) works, and so now there is no need to repeat this. Instead, we shall compare our results with representative works, just as in the case of the tτ motion, for which the phenomenological models are scarce. To represent the breathing model and its "RGM-type" approximant, we chose the results with the D_2 and R force, respectively. We include no "GCM-type" results in these comparisons because, as was mentioned

in sect. 3.4, there is no force to describe all subsystems simultaneously in this model.

Our present results improve on those reported earlier[48,9]) in several respects. In ref.[48]) we showed a breathing-model calculation for $g_{\alpha d}$ and $w_{\alpha d}$, in which the αd separation energy was set correct but the cluster internal states were not realistic (and the Coulomb force was neglected). In ref.[9]) we presented $g_{\alpha d}$ and $f_{\alpha d}$ in a "GCM-type" model (with no Coulomb force) but with the ^{5}He+p clusterization included. The results were reasonable because $E_{\alpha d}$ happened to be almost correct (cf. the caption of fig.4). The effect of the ^{5}He+p clusterization was found to be small, and had the separation energy been readjusted, it would have been even smaller.

Figs. 5 and 6 show amplitudes and potential overlaps for the α+d and the t+τ fragmentation, respectively. The phenomenological functions have been produced by local-potential cluster models as specified by the radial Schrödinger equation

$$(T_{ab} + V_{ab})\, u_{ab}(r) = E_{ab}\, u_{ab}(r) \,. \qquad (4.1)$$

Strictly speaking[49]), the phenomenological counterparts of g_{ab} and w_{ab} are $\hat{A}_{ab}^{1/2} u_{ab}$ and $(E_{ab} - T_{ab})\hat{A}_{ab}^{1/2} u_{ab}$, respectively, where $\hat{A}_{ab}$ is the RGM overlap operator belonging to the cluster internal states $\gamma_1(a)$, $\gamma_1(b)$. Since, however, in actual reaction analyses $\hat{A}_{ab}^{1/2}$ is invariably neglected, we have to regard u_{ab} and $(E_{ab} - T_{ab})u_{ab} = V_{ab} u_{ab}$ as the phenomenological approximants of g_{ab} and w_{ab}.

In fig. 5 we see that the model dependence is more pronounced in $w_{\alpha d}$, especially in the important asymptotic region, than in $g_{\alpha d}$. It is, however, remarkable that the phenomenological model

of Kubo and Hirata (KH)[50]) proposed for the analysis of (^{6}Li,d) reactions are closer to the prediction of the full model than to the simplified one. Based on previous calculations[48,51]), we expect that the KH and D_2 potential overlaps result in α-transfer cross sections differing at most by a factor of 2. Applications of our potential overlaps to (^{6}Li,d) reactions are in progress[52]).

In fig. 6 we see that, in keeping with the difference between the separation energies ($E_{\alpha d} = -1.474$, $E_{t\tau} = -15.794$ MeV), the tτ amplitudes are more localized than the αd amplitudes. It is thus expected that the tτ amplitudes gain contributions mostly from regions of the configuration space that are richly covered by basis states. Thus, although their proper asymptotic fall-off cannot be maintained by an α+d basis, on the whole they are expected to be realistic. The phenomenological curves, due to Hamill and Kunz (HK)[53]), were used to analyse (^{6}Li,t) reactions. These curves imply a t+τ motion that is smeared out to a substantially broader region than that implied by the microscopic calculations. The node positions of both $g_{t\tau}(r)$ and $w_{t\tau}(r)$ as well as the main surface slope of the potential overlap are at larger r values than the respective parts of the αd functions. This is entirely unrealistic and must cause the three-nucleon transfer cross section to be grossly overestimated. This expectation seems to be confirmed by the result that the (^{6}Li,t) cross sections calculated with this phenomenological potential overlap are 80 ÷ 320 times larger than the corresponding zero-range estimates, while for (α,p) transitions between the same states this ratio is close to unity[53]).

Experimentally deduced fragmentation strength functions are

available both for the α+d and t+τ fragmentations. Fig. 7 shows the predictions, for $f_{\alpha d}$, of the D_2 and R forces compared with those extracted from quasielastic ^{6}Li(p,pd) [16,18]) and (α,αd) [17]) knock-out reactions, and fig. 8 shows $f_{t\tau}$ compared with (p,pτ) results[22]). Table 6 contains αd and tτ spectroscopic factors and αd asymptotic normalization constants. (The tails of the tτ amplitudes are not accurate enough to allow an extraction of $\bar{C}_{t\tau}$.)

We see that the predictions of the breathing model for S and $\bar{C}_{\alpha d}$ hardly depend on the force. As for the model dependence of S, we see that the cluster size has more significant effect than the distortion, while for $\bar{C}_{\alpha d}$ this statement should be reversed. For the spectroscopic factors the experimental estimates are somewhat inconsistent with each other, and the breathing model may be said to be consistent with their average, but the discrepancy in $\bar{C}_{\alpha d}$ is significant.

The disagreement in $f_{t\tau}$ is well understood. Roos et al.[22]) have shown that at this low energy (E ≈100 MeV) the "distortions" of the projectile and ejectile waves are significant. (The quotation marks are to distinguish this effect from the distortions of the cluster internal states in ^{6}Li.) The data of fig. 8 are thus to be compared with what is called the "distorted" momentum distribution[22]) rather than with $f_{t\tau}(k)$. The "distorted" momentum distribution is 4 to 6 times smaller than $f_{t\tau}(k)$ around $k = 0$ and has no diffraction minima. It seems thus likely that a "distorted" momentum distribution based on our structure calculations would be consistent with experiment.

The agreement in $f_{\alpha d}$ is much better, and a minor "distortion" effect of the same kind would improve this agreement as well. A

shift of the weight of $f_{\alpha d}(k)$ towards higher $|k|$ values, which seems to be required, could, however, be achieved by an improvement of the structure model as well, viz. by explicit inclusion of short-range nucleon-nucleon correlation in the wave function[45]). This would, at the same time, enhance the extrema of $g_{\alpha d}(r)$ at the expense of its tail, and thus would improve the agreement in $\bar{C}_{\alpha d}$ as well.

However, the recent (e,ed) knock-out data of Ent et al.[25]) published after our preliminary reports[45]) shed some new light on our results (fig. 9). This reaction is more suited to extracting $f_{\alpha d}(k)$ because the "distortion" effects are smaller here[55]). Our results agree with these data better than with any of the knock-out data obtained with nuclear probes. Moreover, it seems very likely that allowance for the slight "distortion" effects would further improve the accord. Indeed, Ent et al. have shown that the "distortions" scale down the theoretical curves in the region $-0.2\ \text{fm}^{-1} < k < 0.5\ \text{fm}^{-1}$ by about a factor of 2/3 and fill up the dip. Such a change on our theoretical curve would certainly bring it even closer to experiment.

The consistency of our $f_{\alpha d}(k)$ with the data of Ent et al. indicates that these data imply an asymptotic normalization constant $\bar{C}_{\alpha d}$ close to our value, 3.3. This apparently contradicts the fact that Ent et al. fit their data with the semi-microscopic fragmentation amplitude of Parke and Lehman[13]), which implies $\bar{C}_{\alpha d} = 2.12$. Comparing this amplitude with ours, one can find that in the tail region they are much closer to each other than the ratio of the two constants $\bar{C}_{\alpha d}$. This makes conceivable why the two fragmentation strengths are not more different. The expla-

nation of the finding that the ratio of the tails differs from that of the normalization constants is that Lehman et al.[12,13] ignore the Coulomb force, and so they have to calculate $\bar{C}_{\alpha d}$ by comparing the tail of $g_{\alpha d}(r)$ with an exponential rather than with a Whittaker function.

Having come across such a prominent Coulomb effect, we made a few exploratory calculations with the Coulomb force neglected and $E_{\alpha d}$ restored by readjustment of the nuclear force. We found that this prescription reduces $\bar{C}_{\alpha d}$ by about a factor of 2/3, just enough to bring our prediction for $\bar{C}_{\alpha d}$ in full agreement with experiment. Lehman et al., however, use force parameters that could be expected to yield the correct $E_{\alpha d}$ only if the Coulomb force were included. Imitating such calculations, we get a reduction by 5/6, which, again, would bring our predictions closer to the experimental data. Based on these tests, it is fair to assume that the apparently perfect reproduction of the experimental $\bar{C}_{\alpha d}$ value by Lehman et al.[12,13] is also an accidental side effect of the neglect of the Coulomb force.

5. Summary, discussion and conclusions

We have described the cluster structure of ^{6}Li in the breathing cluster model in terms of quantities related to cluster fragmentation experiments. We anticipated and subsequently demonstrated the importance of reproducing the correct energies and cluster sizes. It is a major success of the breathing cluster model that it is able to reproduce all these properties with the same simple effective interactions (D_1, D_2, D_2', D_3). A single-clusterization

RGM-type model yields less good cluster energies and sizes and requires more complicated and unconventional interactions (like R). The breathing model with the D forces also reproduces the charge radii [as well as the other electromagnetic properties[45])] of ^{6}Li substantially better than the single-clusterization models. Drawing on these results, we believe that for the fragmentation properties the most reliable force is D_2 [or, alternatively, the "optimized force" of ref.[10]) which is very similar to D_2]. It is nevertheless reassuring that some of the widely used forces give fairly similar results provided that they are modified so as to reproduce E_α, E_d and $E(^6\text{Li})$.

However pre-eminent the breathing model is, the fragmentation properties have changed moderately in comparison with the single-clusterization models. This can be understood by noting that we have always described ^{6}Li and its fragments consistently. Test calculations show that the fragmentation amplitude of an improved ^{6}Li state into a pair of more primitively described clusters differs a great deal from the amplitude of the fragmentation of the equally primitive ^{6}Li state, but the difference is much reduced by introducing the same degree of sophistication into the description of the fragments. Owing to this effect, the αd spectroscopic factor and asymptotic normalization constant in the breathing cluster model remain as high as $S_{\alpha d}$=0.93 and $\bar{C}_{\alpha d}$=3.3. [The earlier[48,6]) figure $S_{\alpha d}$=0.85 was obtained with the V2 force, which is highly irrealistic for the free deuteron.] The tt spectroscopic factor is obtained to be S_{tt}=0.58.

The value $S_{\alpha d}$=0.93 accords with the recent high-energy knock-out data (table 6). Discordant with these results are, first of all,

the three-body calculations (see table 7). Noble's estimate[56], $S_{\alpha d}$=0.54, which is based on dispersion relations combined with the α+p+n picture, suggests that these three-body models are bound to predict such low values of $S_{\alpha d}$ largely independent of the details of the models. The value $S_{\alpha d}$=0.73±0.09, derived from (e,ed) data[25] might also be influenced by the use of the three-body model[13] in the analysis. The other point of major disagreement is in the asymptotic normalization, whose accepted value[54] is $S_{\alpha d}$=2.15±0.06.

In an attempt to explain the discrepancies, we now give a critical comparison of the breathing and three-body models. The exact wave function may be written in the form [cf. (2.1)]

$$\Psi = \sum_k \mathcal{A}\{\psi_k(\alpha)\,\eta_k(\vec{r}_{pn}, \vec{r}_{\alpha d})\}\,, \qquad (5.1)$$

where the spin-isospin coordinates of p and n are suppressed for simplicity.

The three-body model omits the summation over the α internal states and assumes or derives[11] a three-body Schrödinger equation for a function $\tilde{\eta}_1(\vec{r}_{pn}, \vec{r}_{\alpha d})$. The Pauli principle is allowed for merely through inclusion of a potential term, which is either repulsive or contains a projection operator to exclude some states. This model is simple enough to accommodate a realistic force between p and n and to keep as many angular momentum values in the two-particle relative motions as are necessary.

The breathing model, on the other hand, keeps the form (5.1), but replaces $\eta_k(\vec{r}_{pn}, \vec{r}_{\alpha d})$ by a truncated expansion $\sum_\ell \psi_\ell(d)\chi_{k\ell}(\vec{r}_{\alpha d})$. The truncation is consistent with a more schematic nucleon-nucleon force, and confines both $\psi_\ell(d)$ and $\chi_{k\ell}(\vec{r}_{\alpha d})$ to have orbital momentum zero, but within this approximation both may be considered exact. In fact, the breathing model produces 1.6 MeV deeper (i.e. more accurate) binding energy than the microscopic α+p+n model of Krivec and Mihailović[57] if the same force is used[28].

Looking for defects in the breathing model, we quote two estimates for the non-zero angular-momentum components. In our previous work[9] we obtained that a component with orbital momenta $L=1$ both between α and n and between αn and p, coupled to 0, pumps away only 3 % of the wave function from the $(\alpha+d)_{L=0}$ subspace. This is probably an overestimated value because in this model the $(\alpha+d)_{L=0}$ subspace was fairly restricted. (Note that the two subspaces overlap substantially because of the antisymmetrization.) The other estimate, due to Kukulin et al.[58], shows that the weights of all non-zero angular momentum components in the three-body wave functions add up to 4.5 %, out of which 3.4 % being due to the $L=2$ component of the pn motion coupled with αd relative angular momentum zero. Corresponding to this $L=2$ component, however, there is an $L=2$ term in the wave function of the free deuteron as well so that their simultaneous inclusion in both nuclei does not influence $S_{\alpha d}$ appreciably[15]. Thus it seems that the blame for the discrepancy between the two models cannot be put on the breathing model.

As to the three-body model, the neglect of the α excitations is well-known to be an acceptable approximation. The energies and the electromagnetic properties of ^{6}Li being reproduced fairly well, the treatment of the Pauli exclusion also appears to be acceptable in the model subspace of ^{6}Li. Since, however, the fragmentation amplitude is an overlap connecting the state spaces

of ^{6}Li and of its fragments, the straightforward prescription adopted in the three-body model,

$$G_{\alpha d}(\underline{r}) = \int d\underline{r}_{pn}\, \psi_1^*(d)\, \tilde{\eta}_1(\underline{r}_{pn}, \underline{r}) \tag{5.2a}$$

$$= \langle \psi_1(\alpha)\psi_1(d)\delta(\underline{r}-\underline{r}_{\alpha d}) | \psi_1(\alpha)\, \tilde{\eta}_\ell(\underline{r}_{pn}, \underline{r}_{\alpha d})\rangle , \tag{5.2b}$$

does not necessarily work. Indeed, the state vectors in (5.2b) do not show the permutation invariance observable in (4.1). We will now show that this simplification is bound to lead to a serious error.

Let us expand $\tilde{\eta}_1$ as

$$\tilde{\eta}_1(\underline{r}_{pn}, \underline{r}_{\alpha d}) = \sum_\ell \psi_\ell(d)\, \tilde{\chi}_{1\ell}(\underline{r}_{\alpha d}) , \tag{5.3}$$

where $\{\psi_\ell(d)\}$ is a complete orthonormal set of states including the g.s. of the deuteron, $\psi_1(d)$. Because of this orthogonality, the only contribution to $G_{\alpha d}$ comes from $\psi_1(d)$:

$$G_{\alpha d}(\underline{r}) = \tilde{\chi}_{11}(\underline{r}) , \tag{5.4}$$

and hence $S_{\alpha d} = \langle \tilde{\chi}_{11} | \tilde{\chi}_{11} \rangle$. The terms of (5.3) with $\ell \neq 1$ represent the distortion of the deuteron in ^{6}Li. The breathing model calculations show that the weight of the distortion terms is large, and if the three-body model is a good approximation in this respect, which we have no reason to doubt, this weight ought to be large in that model, too. It is therefore not surprising to find that in the three-body model $S_{\alpha d} \ll 1$. The case of an antisymmetrized model is, however, quite different. The terms $\mathcal{A}\{\psi_1(\alpha)\psi_2(d)\chi_{1\ell}(\underline{r}_{\alpha d})\}$ with $\ell > 1$ are not orthogonal to $\mathcal{A}\{\psi_1(\alpha)\psi_1(d)\delta(\underline{r}-\underline{r}_{\alpha d})\}$, and $G_{\alpha d}(\underline{r})$ does gain substantial contributions from them. Indeed, even the

weight of $\mathcal{A}\{\psi_2(\alpha)\psi_1(d)\chi_{21}(\underline{r}_{\alpha d})\}$ is sizeable, and yet $S_{\alpha d}$ is hardly reduced.

This argument can be illustrated by the example given in table V of ref.[10]. [See also fig. 2 of ref.[10].] This contains the weight of each clusterization subspace in the g.s. of ^{6}Li described in the breathing model with a force very similar to D_2. The weights of subspaces $(k,\ell) = (1,2)$ and $(1,3)$ are, 0.131 and 0.389, respectively, and yet the spectroscopic factor of the fragmentation into the g.s. is 0.929. Assuming that the three-body model assigns similar weights to the distortion terms, we would indeed expect $\langle \tilde{\chi}_{11} | \tilde{\chi}_{11} \rangle$ to be around 0.5 ÷ 0.6.

To make the three-body model capable of reproducing $S_{\alpha d}$, one should find the correct relationship between its wave function $\tilde{\eta}_1(\underline{r}_{pn}, \underline{r}_{\alpha d})$ and a microscopic wave function

$$\Psi = \mathcal{A}\{\psi_1(\alpha)\eta_1(\underline{r}_{pn}, \underline{r}_{\alpha d})\} = \int d\underline{\xi} \int d\underline{r}\, \Psi_{\underline{\xi},\underline{r}}\, \eta_1(\underline{\xi}, \underline{r}) , \tag{5.5}$$

where

$$\Psi_{\underline{\xi},\underline{r}} = \mathcal{A}\{\psi_1(\alpha)\delta(\underline{\xi}-\underline{r}_{pn})\delta(\underline{r}-\underline{r}_{\alpha d})\} . \tag{5.6}$$

In this matter we are guided[59] by the correspondence of their normalizations $\langle \Psi | \Psi \rangle = \langle \tilde{\eta}_1 | \tilde{\eta}_1 \rangle (=1)$. This may be rewritten as

$$\langle \eta_1 | \hat{A}_{\alpha pn} | \eta_1 \rangle = \langle \tilde{\eta}_1 | \tilde{\eta}_1 \rangle , \tag{5.7}$$

where $\hat{A}_{\alpha pn}$ is the integral operator defined as

$$\hat{A}_{\alpha pn} F(\underline{\xi}, \underline{r}) = \int d\underline{\xi}' \int d\underline{r}'\, A_{\alpha pn}(\underline{\xi}, \underline{r}; \underline{\xi}', \underline{r}')\, F(\underline{\xi}', \underline{r}') , \tag{5.8}$$

with

$$A_{\alpha pn}(\underline{\xi}, \underline{r}; \underline{\xi}', \underline{r}') = \langle \Psi_{\underline{\xi},\underline{r}} | \Psi_{\underline{\xi}',\underline{r}'} \rangle . \tag{5.9}$$

Eq. (5.7) suggests that

$$\tilde{\eta}_1 \sim \hat{A}_{\alpha pn}^{1/2} \eta_1 \,. \tag{5.10}$$

In fact, $\hat{A}_{\alpha pn}^{1/2}\eta_1$ is distinguished from the other possible inter-cluster "wave functions" by being an eigenfunction of the inter-cluster eigenvalue problem, derivable from the six-nucleon Schrödinger equation $H\Psi=E\Psi$, that belongs to an hermitean hamiltonian, $\hat{A}_{\alpha pn}^{-1/2}\hat{H}\hat{A}_{\alpha pn}^{-1/2}$, where $\hat{H}$ is the integral operator with kernel $\langle \Psi_{\underline{\xi},\underline{x}} | H | \Psi_{\underline{\xi}',\underline{x}'} \rangle$. All three-body models use hermitean hamiltonians, so they must correspond, in some approximation, to this eigenvalue problem. All the more so because it is only in this framework that the invariably neglected three-body forces are small[60].

The function $\hat{A}_{\alpha pn}^{1/2}\eta_1$ is contained in the subspace of the eigenfunctions, of $\hat{A}_{\alpha pn}$, that belong to non-zero eigenvalues. On this subspace $\tilde{\eta}_1 = \hat{A}_{\alpha pn}^{1/2}\eta_1$ can be inverted, to result in

$$\eta_1 = \hat{A}_{\alpha pn}^{-1/2}\tilde{\eta}_1 \,. \tag{5.11}$$

(The function η_1 may as well be defined to contain a component outside this subspace. However, owing to $\mathcal{A}$, the contribution of this component to Ψ vanishes in any case.) By substituting (5.5) and then (5.11) into eq.(4.1), we get

$$G_{\alpha d}(x) = \langle \mathcal{A}\{\psi_1(\alpha)\psi_1(d)\delta(x-x_{\alpha d})\} | \mathcal{A}\{\psi_1(\alpha)\eta_1(x_{pn}, x_{\alpha d})\}\rangle$$
$$= \int d\underline{\xi}\, \psi_1^*(d, x_{pn}=\underline{\xi})\hat{A}_{\alpha pn}\eta_1(\underline{\xi}, x) = \int d\underline{\xi}\, \psi_1^*(d, x_{pn}=\underline{\xi})\hat{A}_{\alpha pn}^{1/2}\tilde{\eta}_1(\underline{\xi}, x) \,. \tag{5.12}$$

This is to be contrasted with eq.(5.2a). It would be reassuring to confirm that with this definition the discrepancy disappears indeed.

In spite of the inexactness of eq.(5.2), it yields amplitudes which are fairly similar to our microscopic ones, apart from their normalization, especially when local potentials and the Coulomb potential are used in the three-body model. As a consequence, the asymptotic normalization of the normalized fragmentation amplitude, $\bar{C}_{\alpha d}/S_{\alpha d}^{1/2}$ is more or less the same in each calculation (see table 7). It is thus obvious that the disagreement between the two models in $\bar{C}_{\alpha d}$ is also rooted just in the improper prescription (5.2). It looks then likely that, with the use of the proper formula (5.12), all calculations would uniformly overshoot the experimental value $\bar{C}_{\alpha d}=2.15$.

As for the resolution of this problem, it may give a hint that all other experimental estimates, though scatter considerably and are believed less reliable, give substantially larger values[61] for $\bar{C}_{\alpha d}$ (except those which neglect the Coulomb potential). On the other hand, it is clear that any additional admixture to the wave function of ^{6}Li is likely to reduce $S_{\alpha d}$, and hence $\bar{C}_{\alpha d}$. However, the near completeness of the microscopic models for cluster distortions of angular momentum zero and the near completeness of the three-body models for higher angular momentum admixtures do not leave much scope for further reductions. Indeed, short-range correlations, by reducing cluster distortion, might even increase $S_{\alpha d}$ slightly. We therefore believe that the true values of $S_{\alpha d}$ and $\bar{C}_{\alpha d}$ can be but a few per cent lower than the values obtained in this work.

The computations involved in this work were carried through during a visit of two of us (RGL and ATK) in Karlsruhe. We are grateful to the KFK for supporting this work and to Prof. G. Schatz and Prof. H. Rebel for their kind hospitality.

Appendix

Exchange mixture in the nuclear potential kernels

From (2.9) it is seen that the potential kernels, i.e. the matrix elements of $V = \sum_{m,n} V(m,n)$ between Φ_{ijk} and $\Phi_{i'j'k'}$ can be expressed in terms of the corresponding unprojected kernels as

$$\langle \Phi_{ijk} | V | \Phi_{i'j'k'} \rangle = \int d\hat{\xi}_k \int d\hat{\xi}'_{k'} Y^*_{LM}(\hat{\xi}_k) \left[\int d\xi \int d\xi' \langle \tilde{\Phi}_{ijk} | V | \tilde{\Phi}_{i'j'k'} \rangle \right] Y_{L'M'}(\hat{\xi}'_{k'}) . \quad \text{(A1)}$$

For simplicity, we assume the form (3.1) for $V(m,n)$. The functions $\tilde{\Phi}$ are Slater determinants. (For brevity, we shall write $\tilde{\Phi}$ for $\tilde{\Phi}_{ijk}$, and $\tilde{\Phi}'$ for $\tilde{\Phi}_{i'j'k'}$.) For the α+N system, where N is a Os cluster containing N nucleons, we can write them in the form

$$\tilde{\Phi} = (N+4)!^{-1/2} \hat{\mathcal{A}} \{\Omega X\}, \qquad \tilde{\Phi}' = (N+4)!^{-1/2} \hat{\mathcal{A}} \{\Omega' X\},$$

where $\hat{\mathcal{A}}$ is the <u>total</u> antisymmetrizer defined as $\sum_p (-)^p P$ and Ω (Ω') and X are space and spin-isospin functions, respectively. For N=α the functions Ω and X may be defined as

$$\Omega = \varphi(x_1)\varphi(x_2)\varphi(x_3)\varphi(x_4)\psi(x_5)\psi(x_6)\psi(x_7)\psi(x_8), \quad \text{(A2)}$$

$$X = \chi_{n\uparrow}(1)\chi_{p\uparrow}(2)\chi_{n\downarrow}(3)\chi_{p\downarrow}(4)\chi_{n\uparrow}(5)\chi_{p\uparrow}(6)\chi_{n\downarrow}(7)\chi_{p\downarrow}(8), \quad \text{(A3)}$$

where

$$\varphi(\underline{x}) = (\beta^\alpha_x/\pi)^{3/4} \exp\left[-\tfrac{1}{2}\beta^\alpha_x(\underline{x}-\underline{z}^\alpha_k)^2\right], \quad \psi(\underline{x}) = (\beta^N_y/\pi)^{3/4} \exp\left[-\tfrac{1}{2}\beta^N_y(\underline{x}-\underline{z}^N_k)^2\right],$$

and the χ are the s.p. spin-isospin eigenvectors with an obvious notation for the z-projections. (The function Ω' is defined with primed quantities analogously.) Omitting the last one, two or three factors of (A 2) and (A 3), we obtain functions corresponding to N=t, d and n, respectively. As the kernels are independent of the projection of the total isospin, the formulae to be derived are also valid for N=τ and p. The formulae for N=n+n and p+p (singlet) can be obtained from those for N=d by exchanging the mixing parameters B and -H in the final result. So the only Os cluster N excluded is the singlet p+n pair.

It is now useful to decompose the unprojected kernel as follows:

$$\langle \tilde{\Phi} | V | \tilde{\Phi}' \rangle = \langle \hat{\mathcal{A}} \{\Omega X\} | V | \Omega' X \rangle = \mathcal{V}_\alpha + \mathcal{V}_N + \mathcal{V}_{\alpha N}, \quad \text{(A4)}$$

with

$$\mathcal{V}_\alpha = \langle \hat{\mathcal{A}} \{\Omega X\} | \sum_{1 \le i < j \le 4} V(i,j) | \Omega' X \rangle,$$

$$\mathcal{V}_N = \langle \hat{\mathcal{A}} \{\Omega X\} | \sum_{5 \le i < j \le N+4} V(i,j) | \Omega' X \rangle,$$

$$\mathcal{V}_{\alpha N} = \langle \hat{\mathcal{A}} \{\Omega X\} | \sum_{i=1}^{4} \sum_{j=5}^{N+4} V(i,j) | \Omega' X \rangle.$$

These are now to be evaluated by letting each $V(i,j)$ act on the right. Owing to the antisymmetry of the bra and to the validity of

$$\langle \hat{\mathcal{A}} \{\Omega X\} | \ldots P^\sigma_{ij} \chi_{t\uparrow}(i) \chi_{t'\downarrow}(j) \ldots \rangle = 0 \quad (t \neq t', \uparrow \neq \downarrow),$$

$$\langle \hat{\mathcal{A}} \{\Omega X\} | \ldots P^\tau_{ij} \chi_{t\uparrow}(i) \chi_{t'\downarrow}(j) \ldots \rangle = 0 \quad (t \neq t', \uparrow \neq \downarrow),$$

each of the operators P^σ_{ij} and P^τ_{ij} can be substituted either by a unit operator or by P^x_{ij}.

For $\mathcal{V}_\alpha$ such a reduction results in

$$\mathcal{V}_\alpha = \langle \Xi | (W+M) \sum_{1 \le i < j \le 4} f(r_{ij}) + (B+H)\left[f(r_{12}) - f(r_{13}) + f(r_{34}) - f(r_{24})\right] | \Omega' \rangle, \quad \text{(A5)}$$

where

$$\Xi \equiv \Xi(x_1,\dots,x_{N+4}) = \langle X | \hat{\mathcal{A}}\{\Omega X\}\rangle.$$

By reducing the determinant $\hat{\mathcal{A}}\{\Omega X\}$, it is easy to show that

$$\begin{aligned}
\Xi &= \mathcal{B}(1,5)\varphi(x_2)\varphi(x_3)\varphi(x_4) && \text{for } N=1,\\
\Xi &= \mathcal{B}(1,5)\mathcal{B}(2,6)\varphi(x_3)\varphi(x_4) && \text{for } N=2,\\
\Xi &= \mathcal{B}(1,5)\mathcal{B}(2,6)\mathcal{B}(3,7)\varphi(x_4) && \text{for } N=3,\\
\Xi &= \mathcal{B}(1,5)\mathcal{B}(2,6)\mathcal{B}(3,7)\mathcal{B}(4,8) && \text{for } N=4,
\end{aligned} \tag{A6}$$

where

$$\mathcal{B}(i,j) = \varphi(x_i)\psi(x_j) - \psi(x_i)\varphi(x_j).$$

It is apparent from the structure of Ξ that in the square brackets in (A 5) the positive and negative terms cancel out pairwise except for $N=2$, when the only simplification is that the contributions of $f(r_{13})$ and $f(r_{24})$ are equal. We can thus write

$$\mathcal{V}_{\omega} = (W+M)\sum_{1\le i<j\le 4}\langle \Xi | f(r_{ij}) | \Omega'\rangle + \delta_{N2}(B+H)\langle \Xi | f(r_{12}) + f(r_{34}) - 2f(r_{13}) | \Omega'\rangle. \tag{A7}$$

Eliminating P^{σ}_{ij} and P^{τ}_{ij}, for $\mathcal{V}_N$, we obtain

$$\mathcal{V}_N = \langle \Xi | (W+M)\sum_{5\le i<j\le N+4} f(r_{ij}) + (B+H)\left[f(r_{56}) - f(r_{59}) + f(r_{78}) - f(r_{68})\right] | \Omega'\rangle,$$

where the terms that contain subscripts larger than $N+4$ are to be understood to be zero. The terms in the square brackets cancel out again, except for $N=2$, when there is just one non-vanishing term. We may thus write

$$\mathcal{V}_N = (W+M)\sum_{5\le i<j\le N+4}\langle \Xi | f(r_{ij}) | \Omega'\rangle + \delta_{N2}(B+H)\langle \Xi | f(r_{56}) | \Omega'\rangle. \tag{A8}$$

The evaluation of $\mathcal{V}_{\omega N}$ is simplified by the relationship

$$\mathcal{V}_{\omega N} = N\langle \hat{\mathcal{A}}\{\Omega X\} | \sum_{i=1}^{4} V(i,5) | \Omega' X\rangle. \tag{A9}$$

For $N=1$ this is trivial. For $N=2$ and 4 the contribution of $\Sigma_i V(i,j)$ is independent of j; this is plausible because such a contribution depends solely on the signs of the spin and isospin projections of nucleon j relative to the other nucleons in the ket, and in these cases the ket is symmetrical in this respect. For $N=3$, however, each nucleon j $(=5,6,7)$ is in a unique position with respect to the others, and a detailed calculation shows that each term $\Sigma_i V(i,j)$ gives a contribution different from the others. It appears accidental that $\langle \Sigma_i V(i,5)\rangle = \langle \tfrac{1}{2}\Sigma_i [V(i,6)+V(i,7)]\rangle$ so that (A9) still holds.

An elimination of P^{σ}_{ij} and P^{τ}_{ij} now yields

$$\begin{aligned}
\mathcal{V}_{\omega N} = N\langle \Xi | W\sum_{i=1}^{4} f(r_{i5}) - M\left[f(r_{15}) - f(r_{25})P^{\sigma}_{25} - f(r_{35})P^{\sigma}_{35} - f(r_{45})P^{\sigma}_{45}\right]\\
+B\left[f(r_{15}) + f(r_{25}) - f(r_{35})P^{\sigma}_{35}\right] - H\left[f(r_{15}) - f(r_{15})P^{\tau}_{15} + f(r_{35})\right] | \Omega'\rangle.
\end{aligned} \tag{A10}$$

To proceed, one can easily verify that each Ξ of (A 6) has the symmetry properties

$$(1 - P^{\sigma}_{1\nu})P^{\tau}_{1\nu} | \Xi\rangle = | \Xi\rangle \qquad (\nu = 2, 3, 4).$$

Multiplying the bra conjugate of this equation by $f(r_{15})|\Omega'\rangle$ from the right, one can derive

$$\langle \Xi | f(r_{\nu 5})P^{\tau}_{\nu 5} | \Omega'\rangle = \langle \Xi | f(r_{15}) - f(r_{\nu 5}) | \Omega'\rangle \qquad (\nu = 2, 3, 4).$$

Applying this equation to (A 10), one obtains

$$\begin{aligned}
\mathcal{V}_{\omega N} = N\big[&(4W - M + 2B - 2H)\langle \Xi | f(r_{15}) | \Omega'\rangle + (W+M)\langle \Xi | f(r_{25})P^{\sigma}_{25} + f(r_{35})P^{\sigma}_{35} + f(r_{45})P^{\sigma}_{45} | \Omega'\rangle\\
&+(B+H)\langle \Xi | f(r_{25}) - f(r_{35}) | \Omega'\rangle\big].
\end{aligned} \tag{A11}$$

A view on (A6) shows that, depending on N, some of the interaction terms in (A11) yield equal contributions. In particular, $\langle \Xi | f(r_{25}) - f(r_{35}) | \Omega'\rangle = 0$ for all cases but $N=2$.

Thus, conferring with (A7) and (A8), we conclude that the nuclear potential kernels of α+N systems only contain the exchange mixtures in the combinations $\xi=W+M$ and $\eta=4W-M+2B-2H$, except that, when N=d, the combination $\zeta=B+H$ also appears. As an exchange of B with $-H$ is equivalent to replacing ξ, ζ, η by $\xi, -\zeta, \eta$, the kernels for α+2p and α+2n also depend just on ξ, ζ and η. As to N being a singlet p+n pair, an analogous derivation reveals that, again, the potential kernel depends solely on ξ, ζ and η.

The evaluation of the kernels is then continued for each system individually by substitution of eq.(A6) into (A7), into (A8) and into (A11) and the latter three equations into (A4). This is still easy to carry through. What remains to be done afterwards is to substitute the formulae of the overlaps $\langle\varphi|\varphi'\rangle$,... and of the two-body matrix elements $\langle\varphi\varphi|f|\varphi'\varphi'\rangle$,... and to perform the integrations in (A1), which are straightforward though tiresome mechanical jobs.

References

1) D.F. Jackson, in Clustering phenomena in nuclei, ed. K. Wildermuth and P. Kramer, vol.3 (Vieweg, Braunschweig, 1983) p.157

2) K. Wildermuth and Y.C. Tang, A unified theory of the nucleus (Vieweg, Braunschweig, 1977)

3) I.V. Kurdyumov, V.G. Neudatchin and Yu.F. Smirnov, Phys. Lett. 31B (1970) 426;
Yu.A. Kudeyarov, I.V. Kurdyumov, V.G. Neudatchin and Yu.F. Smirnov, Nucl. Phys. A163 (1971) 316

4) J.D. Garrett, H.G. Bingham, H.T. Fortune and R. Middleton, Phys. Rev. C5 (1972) 682;
R.A. Lindgren, R.G. Markham and H.W. Fulbright, Phys. Lett. 48B (1974) 209

5) C. Rolfs, Nucl. Phys. A217 (1973) 29

6) R.G. Lovas, Z. Phys. A322 (1985) 589

7) A. Hasegawa and S. Nagata, Prog. Theor. Phys. 45 (1971) 1786

8) H. Walliser and Y.C. Tang, Phys. Lett 135B (1984) 344

9) R. Beck, F. Dickmann and R.G. Lovas, Nucl. Phys. A446 (1985) 703

10) R. Beck, F. Dickmann and R.G. Lovas, Ann. Phys. 173 (1987) 1

11) J. Bang and C. Gignoux, Nucl. Phys. A313 (1979) 119

12) D.R. Lehman and M. Rajan, Phys. Rev. C25 (1982) 2743

13) W.C. Parke and D.R. Lehman, Phys. Rev. C29 (1984) 2319

14) V.T. Voronchev, V.M. Krasnopol'sky, V.I. Kukulin and P.B. Sazonov, J. Phys. G8 (1982) 667

15) V.I. Kukulin, V.M. Krasnopol'sky, V.T. Voronchev and P.B. Sazonov, Nucl. Phys. A417 (1984) 128

16) P. Kitching, W.C. Olsen, H.S. Sherif, W. Dollhopf, C. Lunke, C.F. Perdrisat, J.R. Priest and W.K. Roberts, Phys. Rev. C11 (1975) 420

17) W. Dollhopf, C.F. Perdrisat, P. Kitching and W.C. Olsen, Phys. Lett. 58B (1975) 425

18) D. Albrecht, M. Csatlós, J. Erő, Z. Fodor, I. Hernyes, H. Mu, B.A. Khomenko, N.N. Khovanskij, P. Koncz, Z.V. Krumstein, Yu.P. Merekov, V.I. Petrukhin, Z. Seres and L. Végh, Nucl. Phys. A338 (1980) 477

19) R.G.H. Robertson, P. Dyer, R.A. Warner, R.C. Melin, T.J. Bowles, A.B. McDonald, G.C. Ball, W.G. Davies and E.D. Earle, Phys. Rev. Lett 47 (1981) 1867

20) P.G. Roos, N.S. Chant, A.A. Cowley, D.A. Goldberg, H.D. Holmgren and R. Woody III, Phys. Rev. C15 (1977) 69

21) G.R. Plattner, M. Bornand and K. Alder, Phys. Lett. 61B (1976) 21

22) P.G. Roos, D.A. Goldberg, N.S. Chant, R. Woody III and W. Reichart, Nucl. Phys. A257 (1976) 317

23) A.M. Young, S.L. Blatt and R.G. Seyler, Phys. Rev. Lett. 25 (1970) 1764

24) E. Ventura, C.C. Chang and W.E. Meyerhof, Nucl. Phys. A173 (1971) 1

25) R. Ent, H.P. Blok, J.F.A. van Hienen, G. van der Steenhoven, J.F.J. van den Brand, J.W.A. den Herder, E. Jans, P.H.M. Keizer L. Lapikás, E.N.M. Quint, P.K.A. de Witt Huberts, B.L. Berman, W.J. Briscoe, C.T. Christou, D.R. Lehman, B.E. Norum and A. Saha, Phys. Rev. Lett. 57 (1986) 2367

26) M. Lattuada, F. Riggi, C. Spitaleri and D. Vinciguerra, Nuovo Cimento 83A (1984) 151

27) F.D. Becchetti, D. Overway, J. Jänecke and W.W. Jacobs, Nucl. Phys. A344 (1980) 336;
D.R. Chakrabarty and M.A. Eswaran, Phys. Rev. C25 (1982) 1933

28) R. Beck, F. Dickmann and A.T. Kruppa, Phys. Rev. C30 (1984) 1044

29) H. Horiuchi, Prog. Theor. Phys. Suppl. 62 (1977) 90

30) R.E. Peierls and J. Yoccoz, Proc. Phys. Soc. A70 (1957) 381

31) T. Kajino, T. Matsuse and A. Arima, Nucl. Phys. A413 (1984) 323; A414 (1984) 185;
H. Kanada, T. Kaneko, S. Saito and Y.C. Tang, Nucl. Phys. A444 (1985) 209

32) J.C. Bergstrom, S.B. Kowalski and R. Neuhausen, Phys. Rev. C25 (1982) 1156

33) E. Deumens, doctoral thesis (Antwerp-Brussels, 1982); Nucl. Phys. A423 (1984) 52

34) A.B. Volkov, Nucl. Phys. 74 (1965) 33

35) D.M. Brink and E. Boeker, Nucl. Phys. A91 (1967) 1

36) F. Tanabe, A. Tohsaki and R. Tamagaki, Prog. Theor. Phys. 53 (1975) 677

37) D.R. Thompson and Y.C. Tang, Phys. Rev. 179 (1969) 971

38) D.R. Thompson and Y.C. Tang, Phys. Rev. C8 (1973) 1649

39) D.R. Thompson, M. LeMere and Y.C. Tang, Nucl. Phys. A286 (1977) 53

40) R.C. Barrett and D.F. Jackson, Nuclear sizes and structure (Clarendon, Oxford, 1977) p.146

41) C.R. Ottermann, G. Köbschall, K. Maurer, K. Röhrich, Ch. Schmitt and V.H. Walther, Nucl. Phys. A436 (1985) 688

42) R.E. Brown and Y.C. Tang, Phys. Rev. 176 (1968) 1235

43) K.F. Pál, R.G. Lovas, M.A. Nagarajan, B. Gyarmati and T. Vertse, Nucl. Phys. A402 (1983) 114

44) A.T. Kruppa, R. Beck and F. Dickmann, Phys. Rev. C, in press

45) A.T. Kruppa, R.G. Lovas, R. Beck and F. Dickmann, Phys. Lett. 179B (1986) 317;
R.G. Lovas, A.T. Kruppa, R. Beck and F. Dickmann, to appear in Proc. Int. Conf. on nuclear structure, reactions and symmetries, Dubrovnik, 1986

46) G.R. Plattner and R.D. Viollier, Nucl. Phys. A365 (1981) 8

47) R.G. Lovas, K.F. Pál and M.A. Nagarajan, Nucl. Phys. A402 (1983) 141

48) R.G. Lovas, in Clustering aspects of nuclear structure, ed. J.S. Lilley and M.A. Nagarajan (Reidel, Dordrecht, 1985) p.231

49) R.G. Lovas and K.F. Pál, Nucl. Phys. A424 (1984) 143

50) K.-I. Kubo and M. Hirata, Nucl. Phys. A187 (1972) 186

51) R. Shyam, R.G. Lovas, K.F. Pál, V.K. Sharma and M.A. Nagarajan, J. Phys. G11 (1985) 1199

52) B. Apagyi and T. Vertse, to be published

53) J.J. Hamill and P.D. Kunz, Phys. Lett. 129B (1983) 5

54) M.P. Bornand, G.R. Plattner, R.D. Viollier and K. Alder, Nucl. Phys. A294 (1978) 492

55) C.T. Christou, C.J. Seftor, W.J. Briscoe, W.C. Parke and D.R. Lehman, Phys. Rev. C31 (1985) 250

56) J.V. Noble, Phys. Lett 55B (1975) 433

57) R. Krivec and M.V. Mihailović, J. Phys. G8 (1982) 821

58) V.I. Kukulin, V.M. Krasnopol'sky, V.T. Voronchev and P.B. Sazonov, Nucl. Phys. A453 (1986) 365

59) T. Fliessbach, Z. Phys. A272 (1975) 39

60) S. Nakaichi-Maeda and E.W. Schmid, Z. Phys. A318 (1984) 171

61) L.D. Blokhintsev, I. Borbély and E.I. Dolinsky, Fiz. Elem. Chastits At. Yadra 8 (1977) 1189; Sov. J. Part. Nucl. 8 (1977) 485

Table 1

Energies and rms charge radii[a] of the $A \leq 4$ nuclei with forces of common use

Force	E_d (MeV)	r_d (fm)	E_t (MeV)	r_t (fm)	E_τ (MeV)	r_τ (fm)	E_α (MeV)	r_α (fm)
V1	-0.545	3.655	-7.706	1.893	-6.991	1.912	-27.740	1.694
V2	-0.608	3.541	-8.138	1.909	-7.427	1.928	-28.563	1.702
V3	-0.350	4.295	-7.275	1.851	-6.527	1.872	-28.359	1.619
V4	-0.451	3.812	-7.199	1.824	-6.440	1.844	-28.245	1.606
V5	-0.468	3.855	-7.436	1.915	-6.725	1.935	-27.241	1.693
V6	-0.534	3.673	-7.786	1.907	-7.074	1.927	-27.908	1.697
V7	-0.497	3.798	-7.486	1.922	-6.779	1.942	-27.188	1.700
V8	-0.543	3.662	-7.697	1.914	-6.988	1.933	-27.613	1.701
B_1	-1.016	2.854	-8.384	1.853	-7.660	1.869	-28.460	1.702
B_2	-2.448	2.071	-9.151	1.784	-8.398	1.798	-29.311	1.676
MHN[b]	-7.456	1.505	-9.266	1.735	-8.473	1.749	-30.714	1.606
TT1	-2.226	2.084	-9.861	1.582	-8.920	1.599	-42.233	1.354
TT2	-2.213	2.108	-7.943	1.725	-7.103	1.747	-33.717	1.461
TLT	-2.201	2.105	-6.028	1.874	-5.287	1.898	-25.592	1.618
Experiment	-2.225	2.095(6)[c]	-8.482	1.70(5)[c]	-7.718	1.88(5)[c] 1.976(15)[d]	-28.296	1.674(12)[c] 1.671(14)[d]

[a] The proton charge distribution is represented by a gaussian of squared width 0.43 fm^2.

[b] The weak attractive tensor force not included.

[c] Ref.[40].

[d] Ref.[41].

Table 2

Parameters of the forces designed for cluster distortion models

Symbol	a_1 (fm)	a_2 (fm)	V_1 (MeV)	V_2 (MeV)	ξ	$\eta(^6Li)$	$\eta(^7Li)$
D_1	0.4	1.2	1748.5	-180.82	1.07188	1.16685	1.43328
D_2	0.3	1.42	2706.9	-108.07	1.01997	1.09227	1.30216
D_2'	0.34	1.41	1989	-113.65	1	1.0962	1.2818
D_3	0.44	1.44	1038.5	-117.26	0.94772	1.08872	1.19535

Table 3

Performance of the adjusted forces

Force	E_d (MeV)	r_d (fm)	E_t (MeV)	r_t (fm)	E_τ (MeV)	r_τ (fm)	E_α (MeV)	r_α (fm)	$E(^6Li)$ (MeV)	$r(^6Li)$ (fm)
D_1	-2.225	2.103	-8.482	1.765	-7.709	1.780	-28.296	1.643	-31.994	2.516
D_2	-2.225	2.141	-8.482	1.819	-7.739	1.835	-28.296	1.683	-31.994	2.583
D_2'	-2.237	2.138	-8.462	1.819	-7.719	1.835	-28.308	1.682	-32.018	2.577
D_3	-2.225	2.164	-8.449	1.837	-7.717	1.853	-28.297	1.695	-31.995	2.609
MV1	-2.224	2.212	-7.931	1.883	-7.213	1.902	-28.296	1.690	-31.994	2.634
MV2	-2.225	2.241	-8.031	1.913	-7.322	1.932	-28.296	1.704	-31.994	2.680
MV7	-2.225	2.231	-7.927	1.902	-7.212	1.922	-28.296	1.691	-31.994	2.658
MB_1	-2.224	2.187	-8.314	1.856	-7.591	1.872	-28.296	1.703	-31.991	2.671
MB_2	-2.221	2.136	-8.691	1.800	-7.943	1.814	-28.296	1.682	-31.991	2.610
MMN	-2.225	2.098	-8.196	1.771	-7.419	1.788	-28.296	1.621	-31.994	2.482
MIT	-2.201	2.105	-7.026	1.821	-6.264	1.841	-28.296	1.595	-31.973	2.479
R	-2.225	2.095	-7.594	1.791	-6.876	1.791	-28.275	1.698	-31.974	2.786
		(β^d=0.200)		(β^t=0.390)		(β^τ=0.390)		(β^α=0.502)		
V2	0.579	2.284	-7.185	1.773	-6.459	1.773	-27.957	1.666	-28.851	2.778
		(β^d=0.164)		(β^t=0.400)		(β^τ=0.400)		(β^α=0.528)		
V2	2.450	1.508	-7.185	1.773	-6.459	1.773	-27.445	1.758	-26.468	2.662
		(β^d=0.46)		(β^t=0.400)		(β^τ=0.400)		(β^α=0.46)		

Experiment: $E(^6Li) = -31.994$ MeV, $r(^6Li) = 2.56(10)$ [ref. ^{40}] and see also table 1.

Table 4

Parameters of the modified versions of the standard forces

Symbol	n	ν	a_ν (fm)	V_ν (MeV)	ξ_ν	η_ν
MV1	2	1	0.82	180.88	0.80665	1.06110
		2	1.6	-104.06	0.80665	1.06110
MV2	2	1	1.01	76.319	0.79833	1.01404
		2	1.8	- 75.708	0.79833	1.01404
MV7	2	1	0.81	94.832	0.79692	1.02835
		2	1.8	- 69.128	0.79692	1.02835
MB_1	2	1	0.7	443.05	0.87725	5.82931
		2	1.4	-159.93	0.87725	1.73809
MB_2	2	1	0.6	881.05	1.00391	5.56671
		2	1.2	-243.60	1.00391	1.85851
MMHN[a]	3	1	$3.4^{-\frac{1}{2}}$	1301.6	1.04549	1.78803
		2	$1.127^{-\frac{1}{2}}$	-429.42	1.02559	1.57439
		3	2.5	-4.7189	1.13313	0.44964
MTLT[b]	3	1	$1.487^{-\frac{1}{2}}$	200	1	1.35230
		2	$0.639^{-\frac{1}{2}}$	-178	0.5	0.61707
		3	$0.465^{-\frac{1}{2}}$	- 95.461	0.5	0.73523

[a] Central part only.

[b] $u = 0.94092$; $\xi_3 + \zeta_3 = 0$, cf. eq. (3.6).

Table 5

Parameters of a force constructed for a conventional "RGM-type" model

Symbol	n	ν	a_ν (fm)	V_ν (MeV)	ξ_ν	η_ν
R	2	1	0.45	3036.6	0.10249	0.19022
		2	1.89	-125.43	0.39161	0.72682

Table 6

Fragmentation constants of ^{6}Li

Model	Force	$E_{\alpha d}$ (MeV)	$S_{\alpha d}$	$\bar{C}_{\alpha d}$	E_{tr} (MeV)	S_{tr}
full	D_1	-1.474	0.926	3.14	-15.803	0.574
full	D_2	-1.474	0.930	3.30	-15.774	0.580
full	D_2'	-1.474	0.930	3.30	-15.837	0.579
full	D_3	-1.474	0.929	3.35	-15.829	0.581
full	MV1	-1.474	0.921	3.42	-16.850	0.579
full	MV2	-1.474	0.921	3.56	-16.641	0.571
full	MV7	-1.474	0.920	3.51	-16.855	0.571
full	MB_1	-1.471	0.927	3.51	-16.086	0.557
full	MB_2	-1.474	0.929	3.36	-15.357	0.558
full	MMHN	-1.474	0.919	3.08	-16.379	0.577
full	MTLT	-1.475	0.912	3.10	-18.683	0.564
"RGM-type"	R	-1.474	0.973	3.84	-17.504	0.462
"RGM-type"	V2	-1.474	0.974	3.72	-15.794	0.476
"GCM-type"	V2	-1.474	1.076	3.71	-15.794	0.722
Experiment		-1.474	0.78±0.1[a] 1.08[a,b] 1.05±0.12[b] 1.08±0.1[c] 1.31±0.18[c] 0.73±0.09[d]	2.15±0.06[e]	-15.794	(0.73÷1.35) $S_{\alpha d}$ [f]

a) Kitching et al.[16])
b) Dollhopf et al.[17])
c) Albrecht et al.[18])
d) Ent et al.[25])
e) Bornand et al.[54])
f) Roos et al.[22])

Table 7

Theoretical αd fragmentation constants

Model	$S_{\alpha d}$	$\bar{C}_{\alpha d}$	Coulomb corrected[a] $\bar{C}_{\alpha d}$	$\bar{C}_{\alpha d}/S_{\alpha d}^{1/2}$
Three-body[b]	0.52	2.6	2.6	3.61
Three-body[c]	0.654	2.182	2.62	3.24
Three-body[d]	0.613	2.034	2.44	3.12
Three-body[e]	0.66			
Three-body[f]	0.753	2.71	2.71	3.12
Breathing[g]	0.93	3.3	3.3	3.42

a) Multiplied by 1.2 when no Coulomb force was used. See sect.4.3.
b) Bang and Gignoux[11]).
c) Lehman and Rajan[12]).
d) Parke and Lehman[13]).
e) Voronchev et al.[14]).
f) Kukulin et al.[15]).
g) Present work.

Figure captions

Fig. 1. The αd fragmentation amplitude in the breathing model with the D forces.

Fig. 2. The αd fragmentation amplitude in the breathing model with some of the M forces. For reference, the D_2 curve is also shown.

Fig. 3. Model dependence of the αd fragmentation amplitudes. For the restricted models see sect. 3.4.

Fig. 4. Energetically adjusted versus non-adjusted αd fragmentation amplitudes. The $E_{\alpha d}$ values in MeV: -1.474 (MV2, correct value), 0.165 (V2), 0.608 (V2, "RGM-type"), -0.919 (V2, "GCM-type"), -1.675 (V2, "GCM-type", no Coulomb).

Fig. 5. Microscopic versus phenomenological (KH) αd fragmentation amplitudes (a) and potential overlaps (b). KH stands for Kubo and Hirata[50]).

Fig. 6. Microscopic versus phenomenological (HK) tτ fragmentation amplitudes (a) and potential overlaps (b). HK stands for Hamill and Kunz[53]).

Fig. 7. Calculated αd fragmentation strengths compared with those extracted from knock-out experiments induced by nuclear probes [Albrecht et al.[18]), Kitching et al.[16]), Dollhopf et al.[17])].

Fig. 8. Calculated and extracted[22]) tτ fragmentation strengths.

Fig. 9. Calculated αd fragmentation strengths compared with that extracted from an (e,ed) experiment[25]).

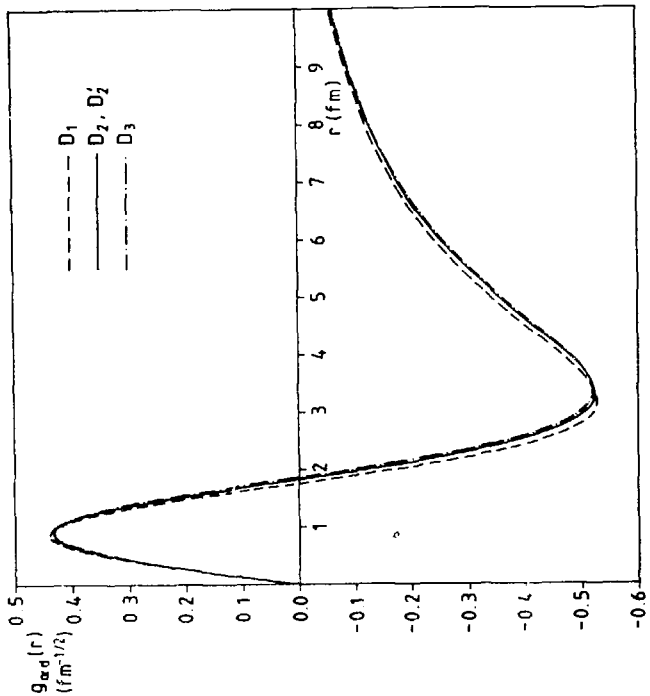

Fig. 1

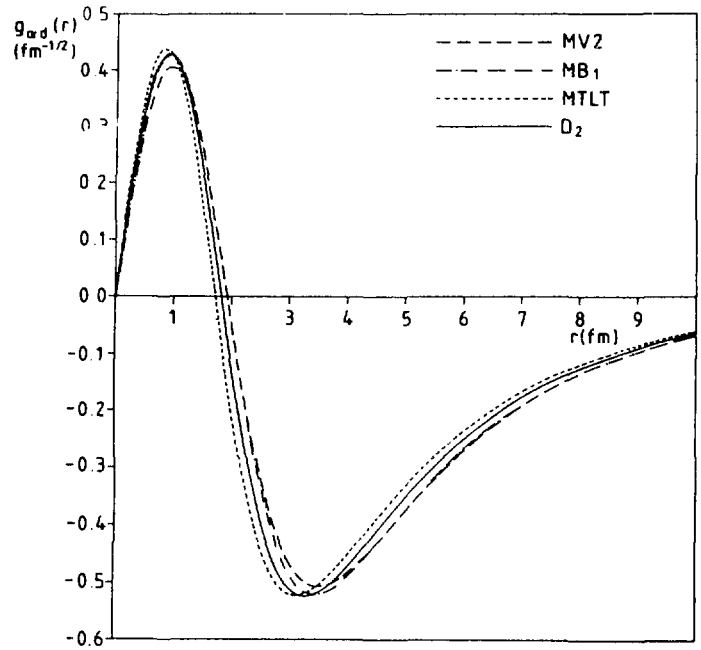
$g_{\alpha d}(r)$ $(fm^{-1/2})$
MV2
MB_1
MTLT
D_2
r(fm)

Fig. 2

Fig. 3

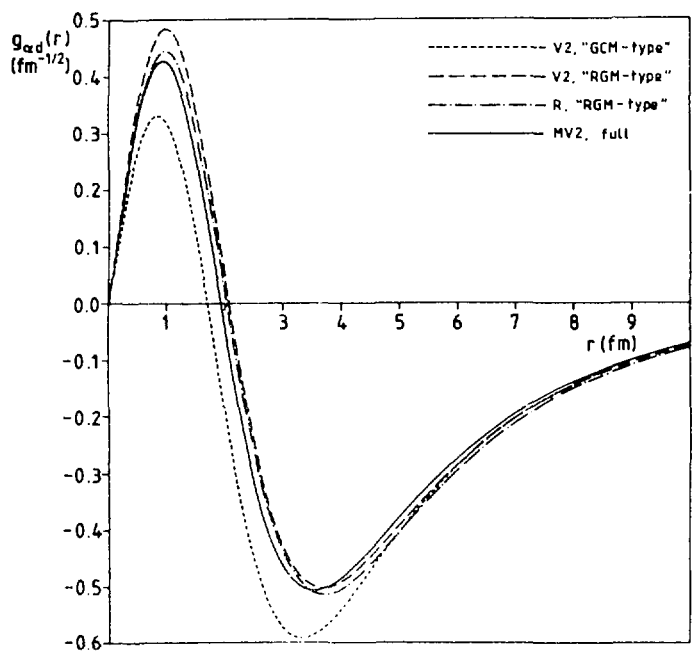
$g_{\alpha d}(r)$ $(fm^{-1/2})$
V2, "GCM-type"
V2, "RGM-type"
R, "RGM-type"
MV2, full
r (fm)

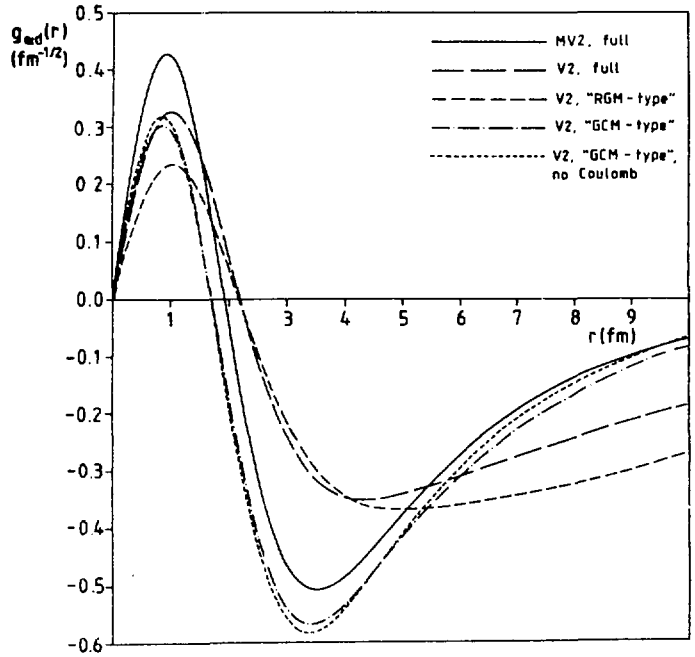
$g_{\alpha d}(r)$ $(fm^{-1/2})$
MV2, full
V2, full
V2, "RGM-type"
V2, "GCM-type"
V2, "GCM-type", no Coulomb
r(fm)

Fig. 4

Fig. 5

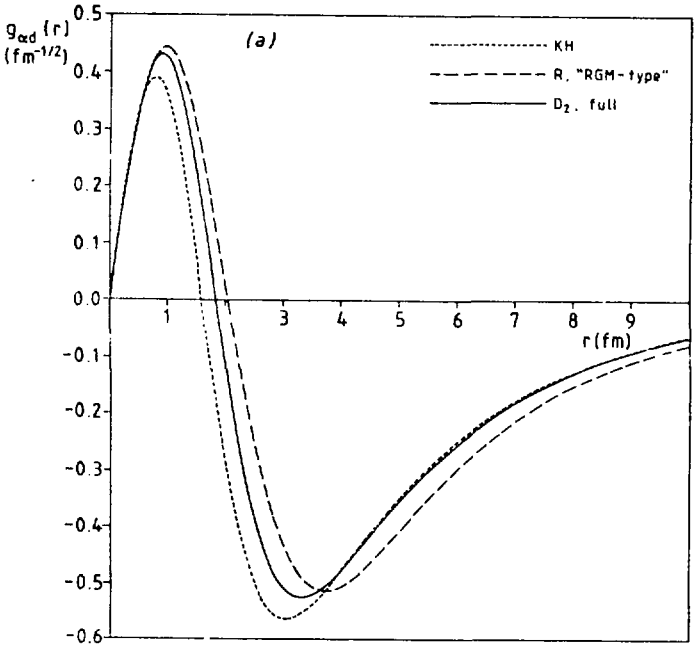
$g_{\alpha d}(r)$ $(fm^{-1/2})$
(a)
KH
R, "RGM-type"
D_2, full
r(fm)

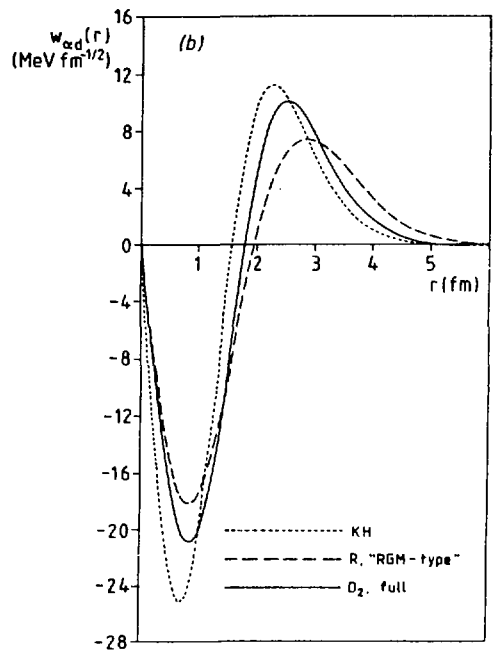
$W_{\alpha d}(r)$ (MeV $fm^{-1/2}$)
(b)
KH
R, "RGM-type"
D_2, full
r(fm)

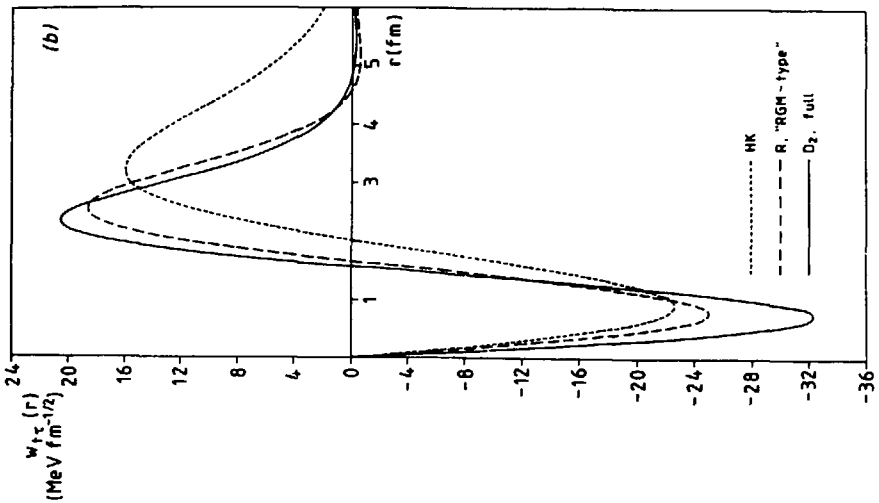
(b)
HK
R, "RGM-type"
D_2, full
r (fm)
$w_{t\tau}(r)$ (MeV fm$^{-1/2}$)

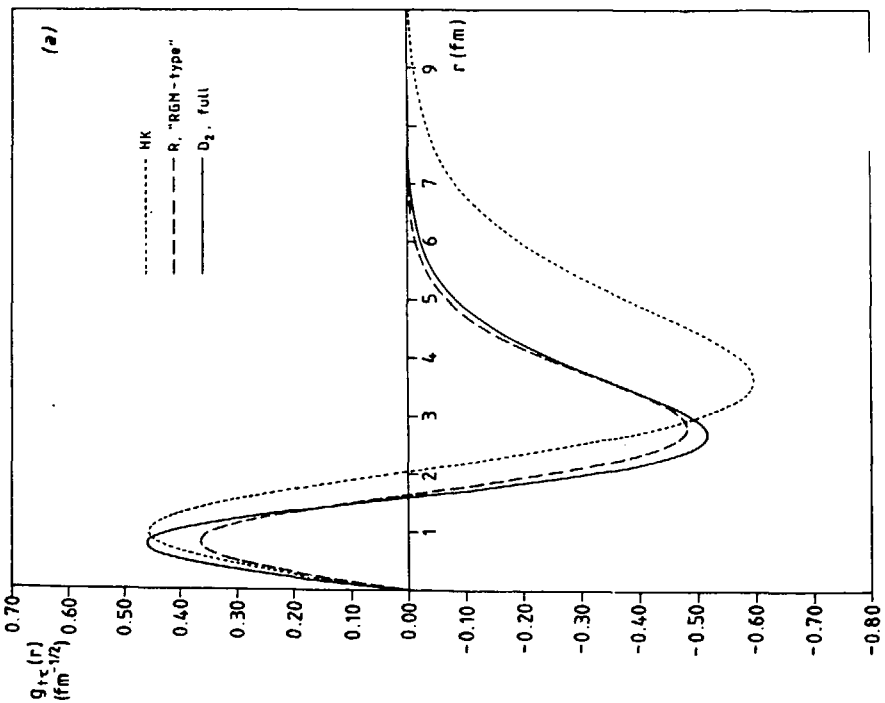
(a)
HK
R, "RGM-type"
D_2, full
r (fm)
$g_{t\tau}(r)$ (fm$^{-1/2}$)

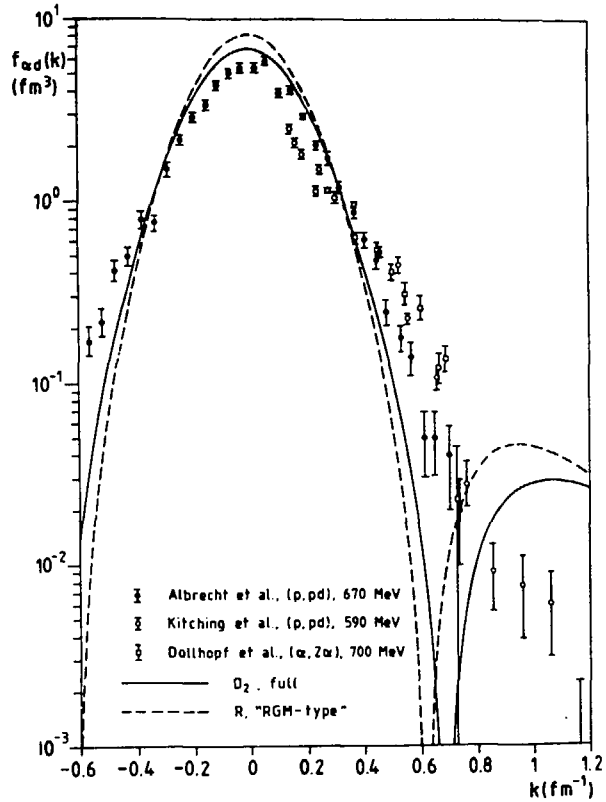
$f_{\alpha d}(k)$ (fm^3)
Albrecht et al., (p,pd), 670 MeV
Kitching et al., (p,pd), 590 MeV
Dollhopf et al., (α,2α), 700 MeV
D_2, full
R, "RGM-type"
k(fm^{-1})

Fig. 7

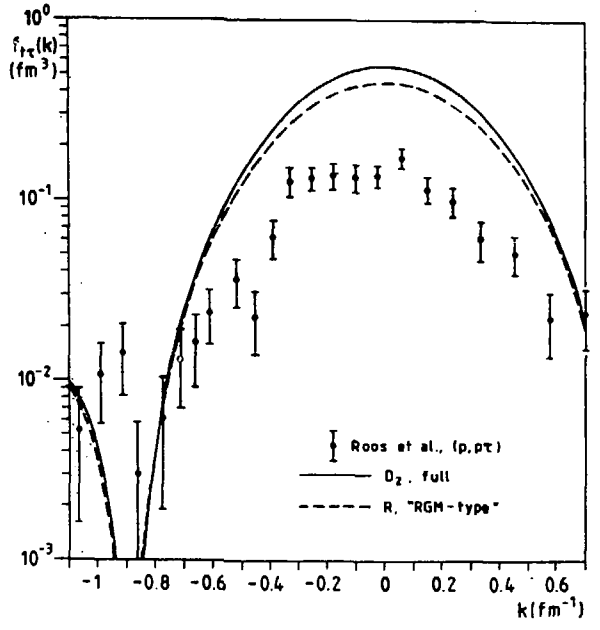
10^0
$f_{t\tau}(k)$
(fm^3)
10^{-1}
10^{-2}
10^{-3}
-1
-0.8
-0.6
-0.4
-0.2
0
0.2
0.4
0.6
$k(fm^{-1})$
Roos et al., (p,pτ)
D_2, full
R, "RGM-type"

Fig. 8

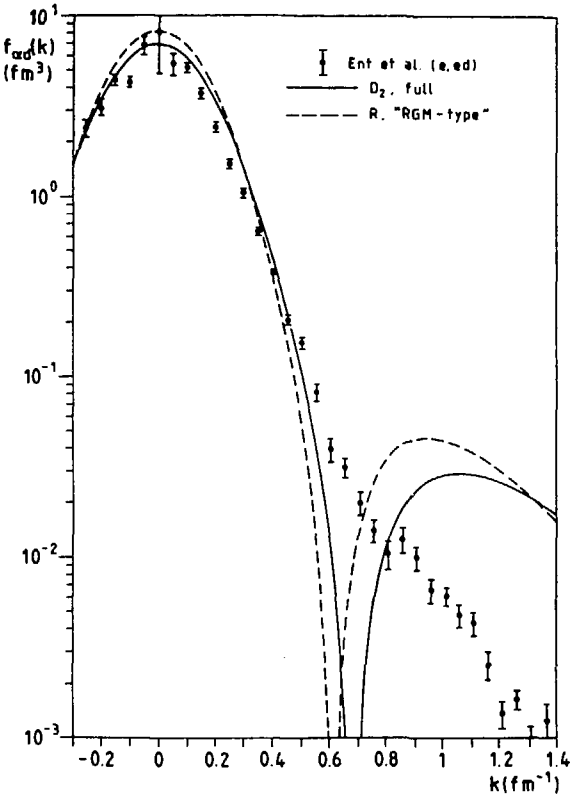
10^1
$f_{\alpha d}(k)$
(fm^3)
10^0
10^{-1}
10^{-2}
10^{-3}
-0.2
0
0.2
0.4
0.6
0.8
1
1.2
1.4
$k(fm^{-1})$
Ent et al. (e,ed)
D_2, full
R, "RGM-type"

Fig. 9